A COMPARISON OF CALCULATED AND MEASURED CF-252 NEUTRON SPECTRA

A Thesis

Submitted to the Graduate Faculty of the
Louisiana State University and
Agricultural and Mechanical College
in partial fulfillment of the
requirements for the degree of

Master of Science

in

The Department of Nuclear Engineering

by

Jim Emanuel Morel
B.S., Louisiana State University, 1972

May, 1974

DEDICATED TO

my family

ACKNOWLEDGEMENT

This work was made possible through the efforts of many people. The author wishes to express his deepest appreciation to Dr. John C. Courtney, Dr. Frank A. Iddings, and Dr. Robert C. McIlhenny for the indispensable assistance which they rendered during the course of this work. Mr. Jim Robert was very helpful in assisting with the preparation of input data for the ANISN computer code. Mr. Malcolm McNaylor of the LSU Computer Research Center was kind enough to spend many hours in solving some of the problems which arose in the running of ANISN.

Special thanks must be given to Mr. Wayne Rhodes and Mr. Ward Engle, Jr. of Oak Ridge National Laboratory. Without the assistance given by these two gentlemen, erroneous conclusions would have undoubtedly resulted in this work.

TABLE OF CONTENTS

LIST OF TABLES

PAGE

TABLE

LIST OF FIGURES

ABSTRACT

To support the operations of the Louisiana State University Californium Demonstration Center, a quantification of the neutron levels associated with Cf-252 radioisotopic sources was desired. In particular, absolute values of neutron spectra would be valuable to many investigators. Measurements were made at three energy levels and compared to the results of more detailed calculations.

Thermal ($E < 0.414$ ev), resonance ($E \simeq 1.45$ ev), and fast ($E > 3$ Mev) neutron fluxes were measured with activation foil techniques 1.75 centimeters from a point source of Cf-252 for three arrangements of water, air, and gold about the source. A series of P_3, S_{16}, 23-energy group calculations were made for the three arrangements with the one-dimensional discrete-ordinates neutron transport code, ANISN. The agreement between calculated and measured fast neutron fluxes is excellent, but agreement between the calculated and measured thermal and resonance neutron fluxes is poor. The use of higher order discrete-ordinates approximation with the ANISN code is indicated for the accurate calculation of thermal neutron fluxes at points near the source in problems treating a point source of Cf-252 in an infinite water medium.

CHAPTER I

INTRODUCTION

Measurements of neutron spectra are lengthy and generally lacking in detail when made with activation foils.[1] Good absolute values of thermal neutron flux are possible because the thermal activation cross-sections are well known as a function of energy, and the thermal neutron spectrum in water is closely approximated by a Maxwellian distribution. But measurements of the resonance neutron flux are generally poor because the effective resonance integrals are difficult to calculate, and the flux that is measured only describes a small portion of the total resonance neutron flux. Fast neutron flux measurements depend upon threshold reactions, and thus yield the average flux value over the large range of energy above the threshold value. The threshold energies themselves are poorly defined because the cross-sections do not increase discontinuously at what would truly be the threshold energy, but rather increase fairly rapidly over a finite energy range. Consequently, a complete description of the neutron spectrum is not obtainable with activation foil techniques.

In recent years, sophisticated computer codes have been developed to solve the Boltzmann transport equation numerically. In theory, the detail and accuracy of a solution is limited only by the memory space and running time available.[2] Thus an appropriate code with accurate input data can give detailed spectral information which is difficult if not impossible to measure.

The primary object of this work is to compare calculations of the computer code ANISN[3] with measurements made in several arrangements of water, air, and gold about a point source of Cf-252 in what is essentially an infinite medium of water. The suitability of ANISN for deep penetration problems is well known, but information on its accuracy at points near the source is not well documented.

CHAPTER II

THE ANISN CODE

ANISN uses the discrete-ordinates method to solve the one-dimensional Boltzmann transport equation numerically in slab, spherical, or cylindrical geometry. Sources may be fixed, fission, or a subcritical combination of the two. Scaler and angular fluxes are computed for all problems, and any one of several criticality parameters may be calculated for reactor problems. A complete description of the code is given in Reference (3). A brief description of the Boltzmann transport equation and the discrete-ordinates method is given in Appendix A of this thesis.

Because ANISN is a one-dimensional code, all point source systems are represented with a spherically symmetric model. For instance, if a source were to be shielded with two concentric cylinders of lead and graphite, the representative ANISN model would consist of two concentric spheres as shown in Figure 1. The three ANISN models that were used are shown in Figures 2, 3, and 4 respectively.

The first model consists of a point source of Cf-252 surrounded by a sphere of water with a radius of 30 centimeters. The second model is identical to the first except that a spherical ring of air with an inner radius of 1.2 centimeters and an outer radius of 2.4 centimeters is centered about the source. Two spherical gold rings, each with a thickness of 0.762 millimeters, are placed respectively at the inner and outer boundries of the air ring to complete the third and final model treated in this investigation.

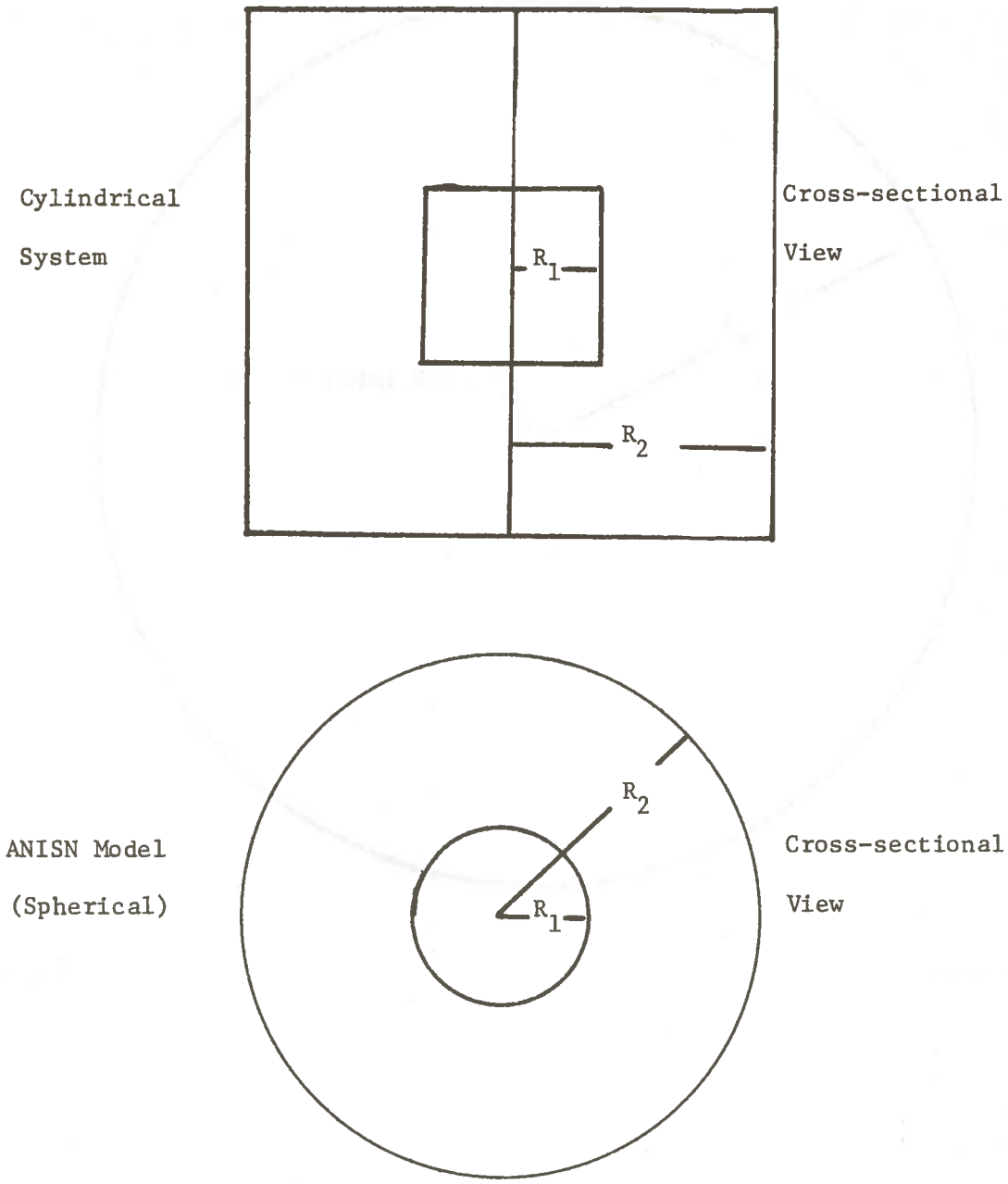

FIGURE 1. The ANISN Model for a Cylindrical System

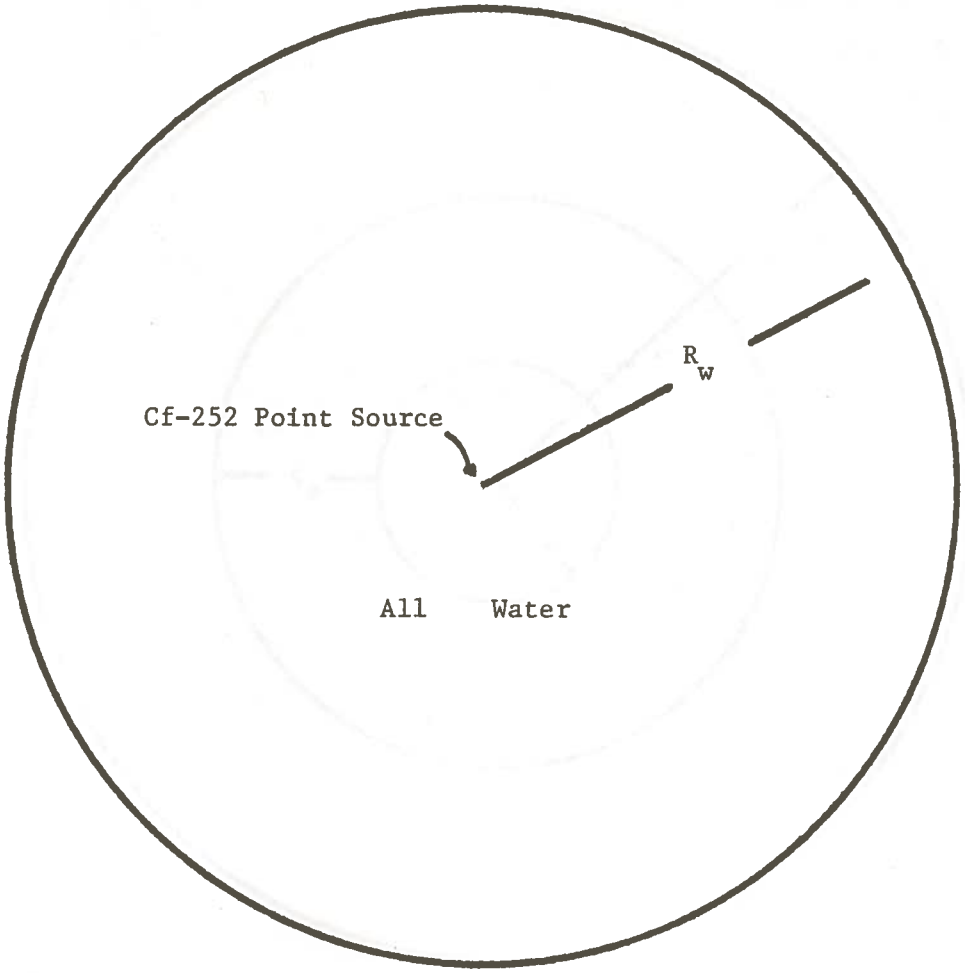

R_w = 30 cm

FIGURE 2. The ANISN Model for System One.

A point source of Cf-252 is at the center of the sphere.

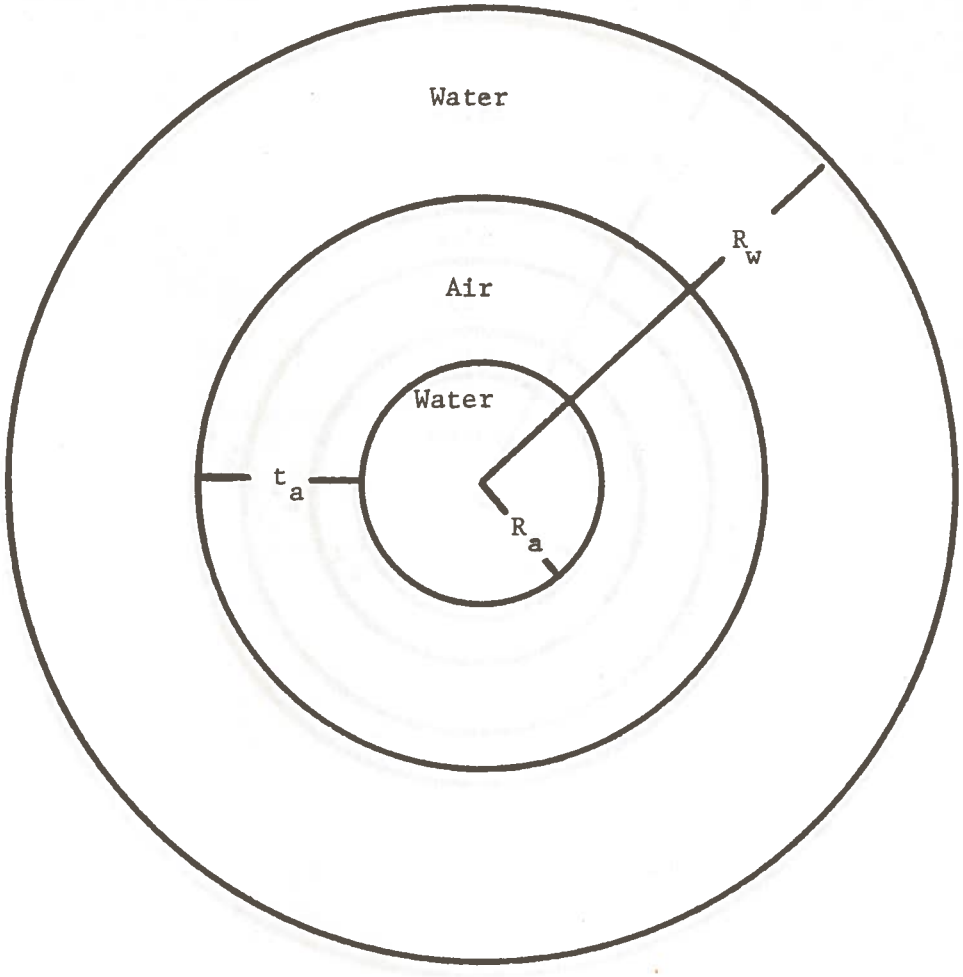

R_w = 30 cm t_a = 1.2 cm

R_a = 1.2 cm

FIGURE 3. The ANISN Model for System Two

A point source of Cf-252 is at the center of the sphere.

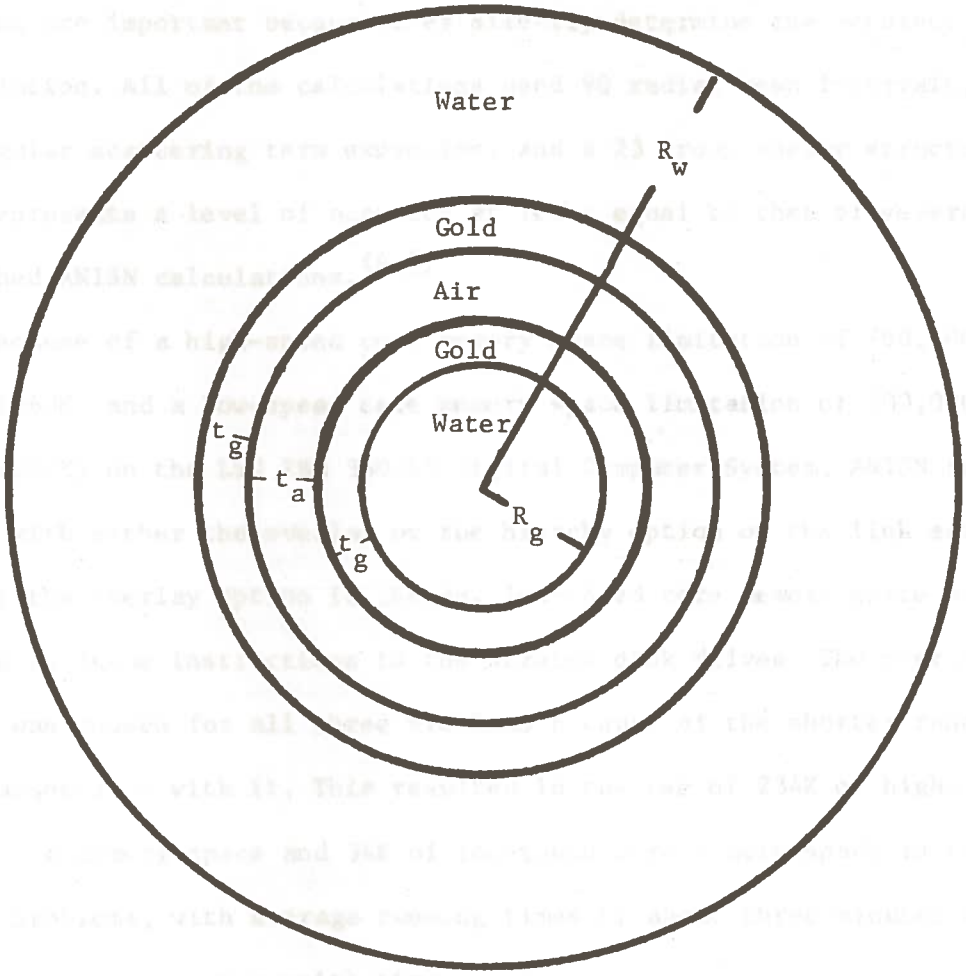

R_w = 30 cm

R_g = 1.2 cm

t_g = 0.762 mm

t_a = 1.0476 cm

FIGURE 4. The ANISN Model for System Three

The various approximation parameters in a discrete-ordinates calculation are important because they directly determine the accuracy of the solution. All of the calculations used 90 radial mesh intervals, a P-3 angular scattering term expansion, and a 23 group energy structure. This represents a level of accuracy at least equal to that of several published ANISN calculations.(4,5)

Because of a high-speed core memory space limitation of 260,000 bytes (260K) and a low-speed core memory space limitation of 200,000 bytes (200K) on the LSU IBM 360/65 Digital Computer System, ANISN must be run with either the overlay or the hiarchy option of the link editor. If the overlay option is chosen, low-speed core memory space must be used to issue instructions to the scratch disk drives. The overlay option was chosen for all three problems because of the shorter running times associated with it. This resulted in the use of 234K of high-speed core memory space and 34K of low-speed core memory space in each of the problems, with average running times of about three minutes of CPU (central processing unit) time.

A complete listing of the input data for the first problem is given in Appendix B.

CHAPTER III

IRRADIATOR DESIGN AND EXPERIMENTAL TECHNIQUE

A basic irradiation system was constructed as shown in Figures 5 and 6. It was primarily designed to allow the measurement of the neutron spectrum at a distance of 1.75 cm from a point source of Cf-252 in the large water tank of the Cf-252 Demonstration Facility. Secondary design criteria included the ability to position a cylindrical ring of air about the source, and the ability to position small gold filtering foils about the activation foils.

Plexiglass* was chosen as the construction material because its high hydrogen content gives it nuclear properties very similar to those of water. Thus the basic system eventually maintains the normal hydrogenous neutron spectrum about the source. A source guide was installed becaused it reduces source transfer times from a range of about 10 seconds to a range of less than one second. The platform was equipped with 18 cm vertical supports to reduce the effect on the neutron spectrum near the source by the non-hydrogenous tank floor. The minimum distance of a path for a neutron traveling from the source to the tank floor and back to the point of flux measurement is about 34 cm. Since the migration length for fission neutrons in water is about 6.22 cm, it is very unlikely that any neutrons which come in contact with the tank floor will reach the point of flux measurement before being absorbed.

---

* Registered trade mark for acrylic sheet; Rohm and Haas Co.

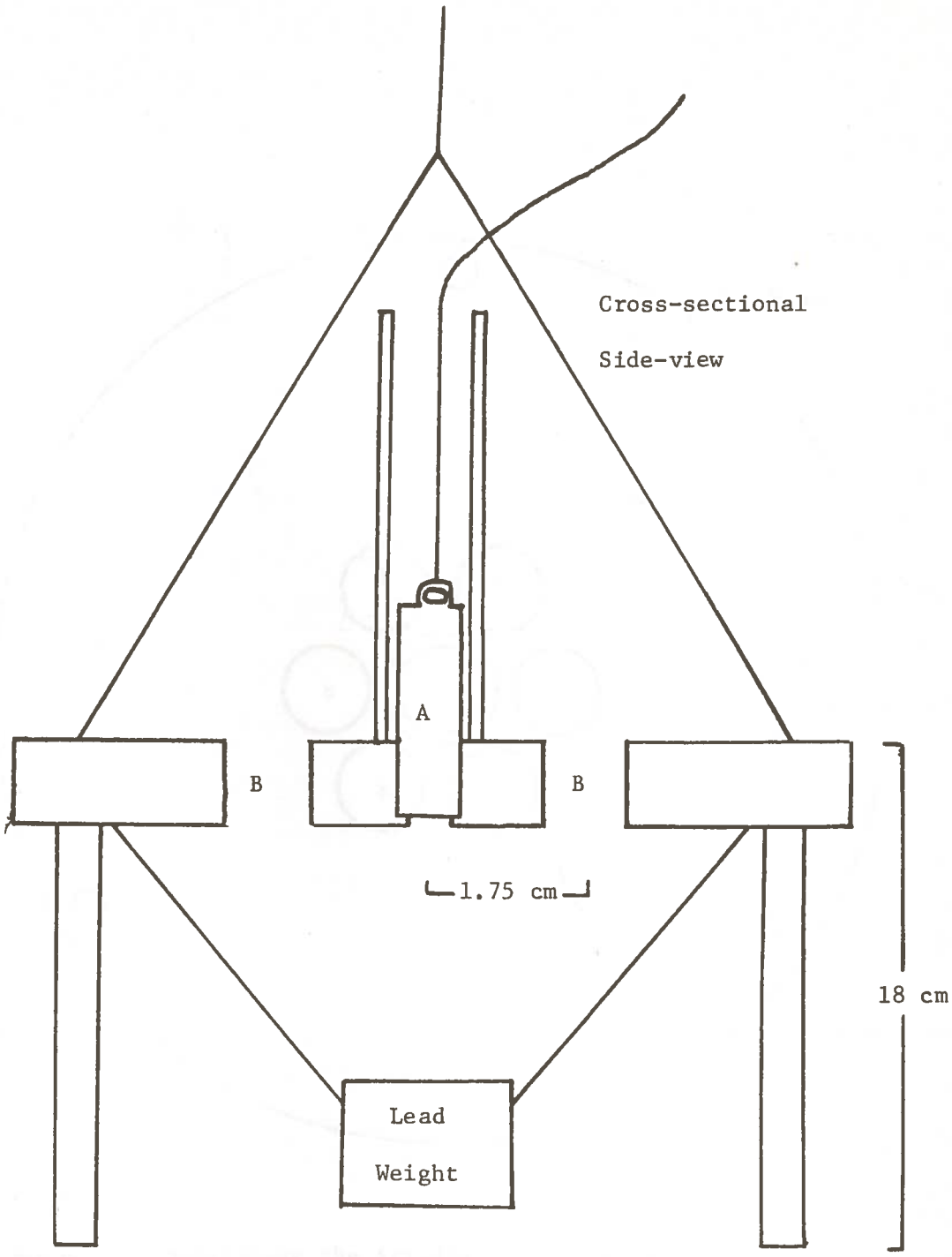

A = Cf-252 source.

B = Holes for positioning the irradiation containers.

FIGURE 5. The Basic Irradiation System - View One

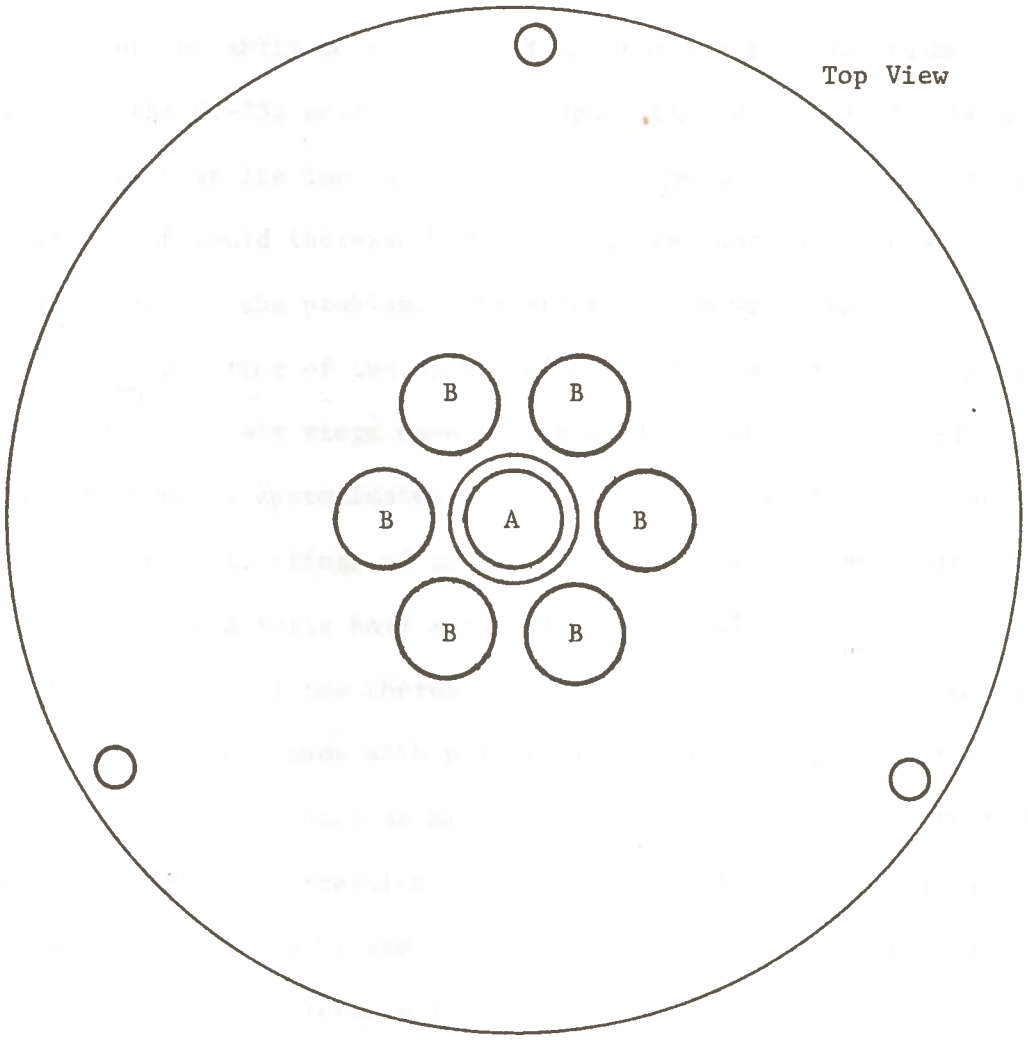

A = Cf-252 source.

B = Holes for positioning the irradiation containers.

FIGURE 6. The Basic Irradiation System - View Two

A set of measurements was made for each of three system arrangements. These arrangements are shown in Figures 7, 8, and 9 respectively. The first ANISN model is essentially identical to the first system except that the ANISN model does not account for the zirconium encapsulation of the Cf-252 source. The encapsulation was neglected because it was felt that its inclusion would only have a small effect on the solution, but would increase both the required core storage space and running time for the problem. The second ANISN model approximates the cylindrical air ring of the system with a spherical air ring. Both the model and system air rings have a volume of 50 cubic centimeters. The third ANISN model approximates the two parallel gold foils in the system with two concentric rings of gold. Both the spherical gold rings and the parallel gold foils have a thickness of 0.762 millimeters.

Measurements of the thermal neutron flux and the 1.45 ev neutron resonance flux were made with pure indium foils. Standard activation foil techniques were used as described in reference (6). Corrections were made for flux depression in the indium foils and for perturbations of the resonance flux by the cadmium covers. These correction factors were obtained from reference (7).

The foils were counted using a Harshaw type 12-S-12, 3 inch by 3 inch NaI(Tl) Integral Line Detector assembly, a Hewlett-Packard Model 6515-A high voltage supply, an Ortec Model 485 amplifier and a TMC Model 401-D, 400 channel analyzer. The foils were counted on the surface of the plexiglass beta particle shield as shown in Figure 10. This resulted in an average source to detector distance of about 1.5

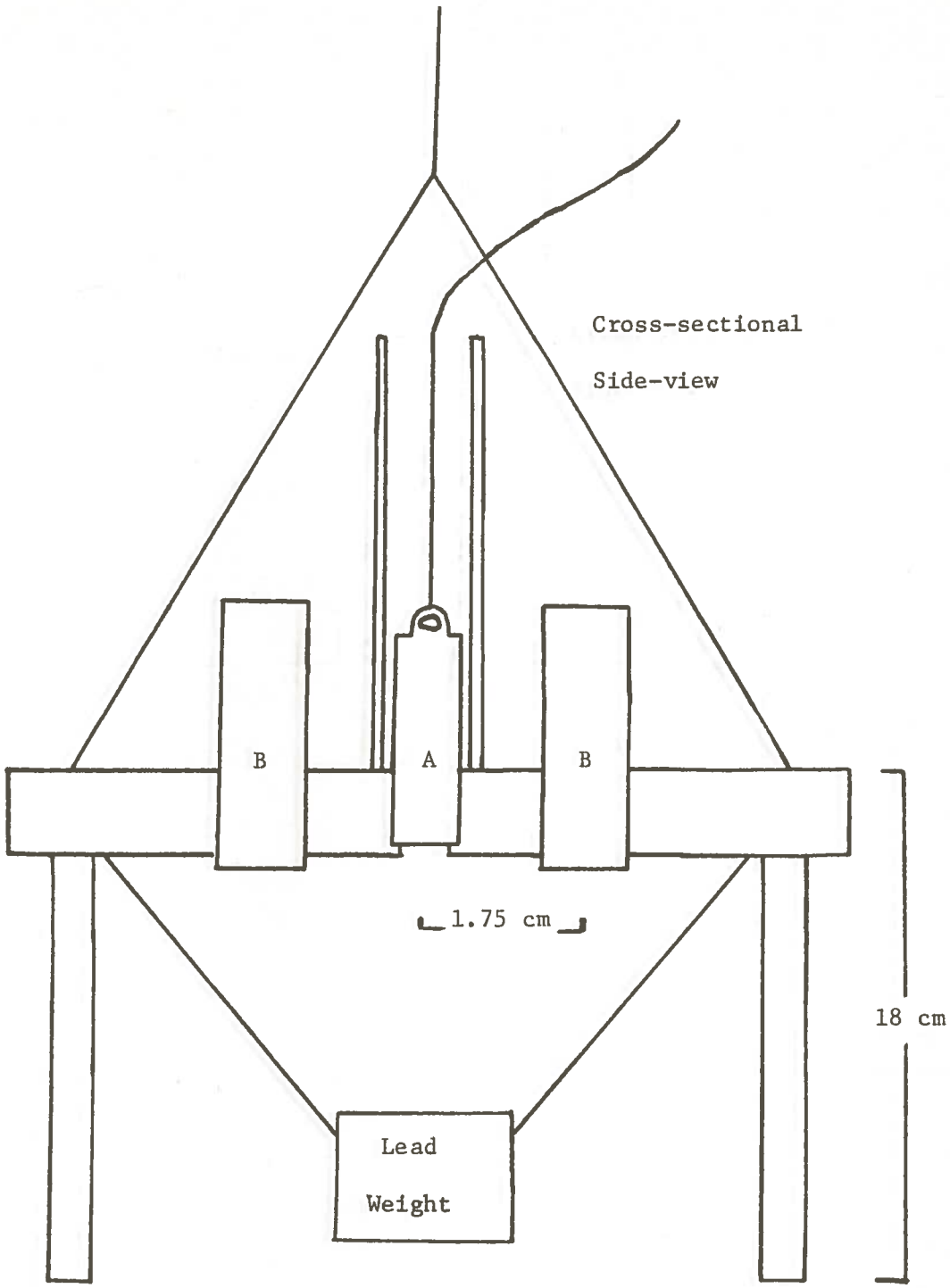

A = Cf-252 source.

B = Irradiation containers, five containing water alone, one containing water and the activation foils.

FIGURE 7. The First Irradiation System (Water Only)

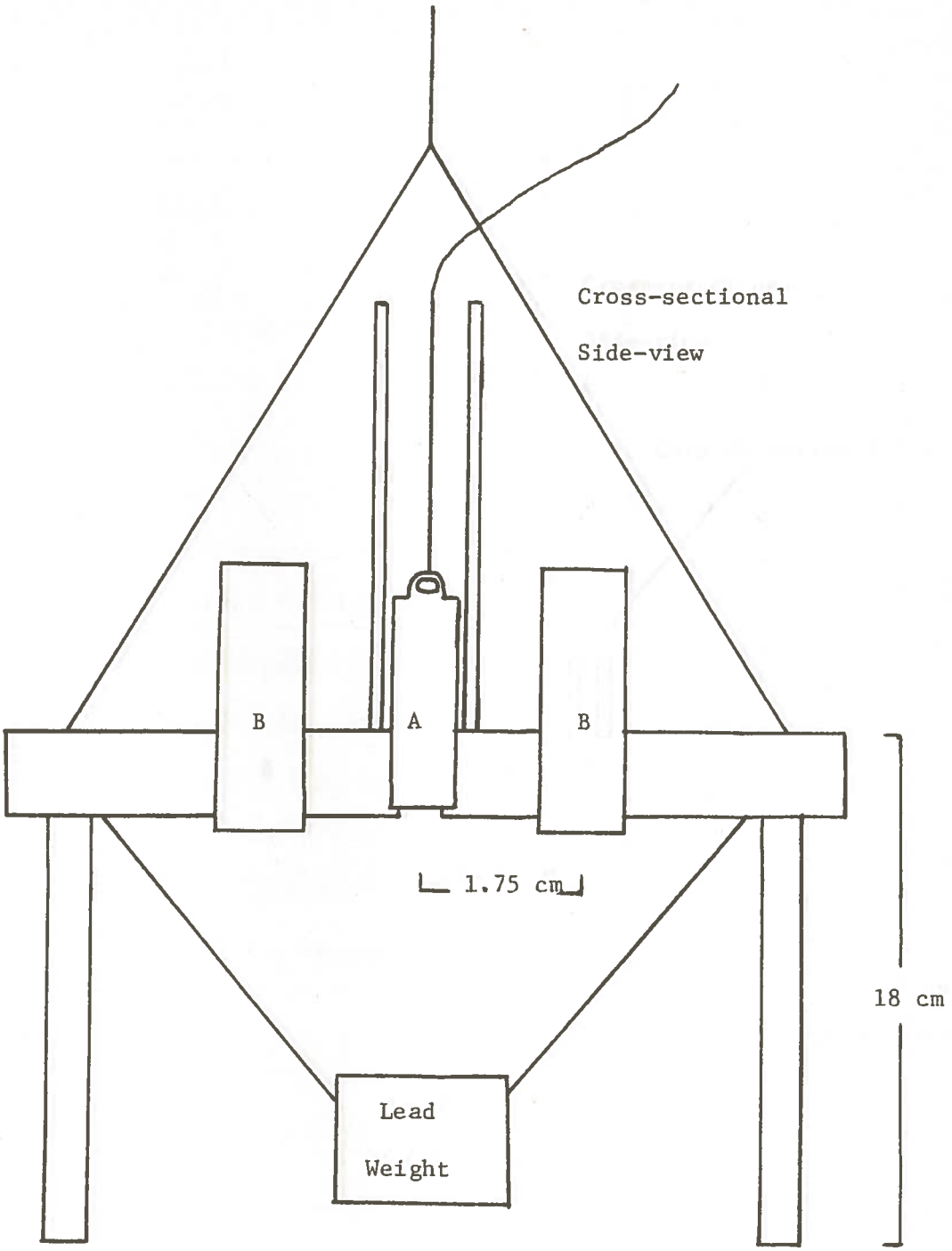

A = Cf-252 source.

B = Irradiation containers, five containing air alone, one containing air and the activation foils.

FIGURE 8. The Second Irradiation System (Water and Air)

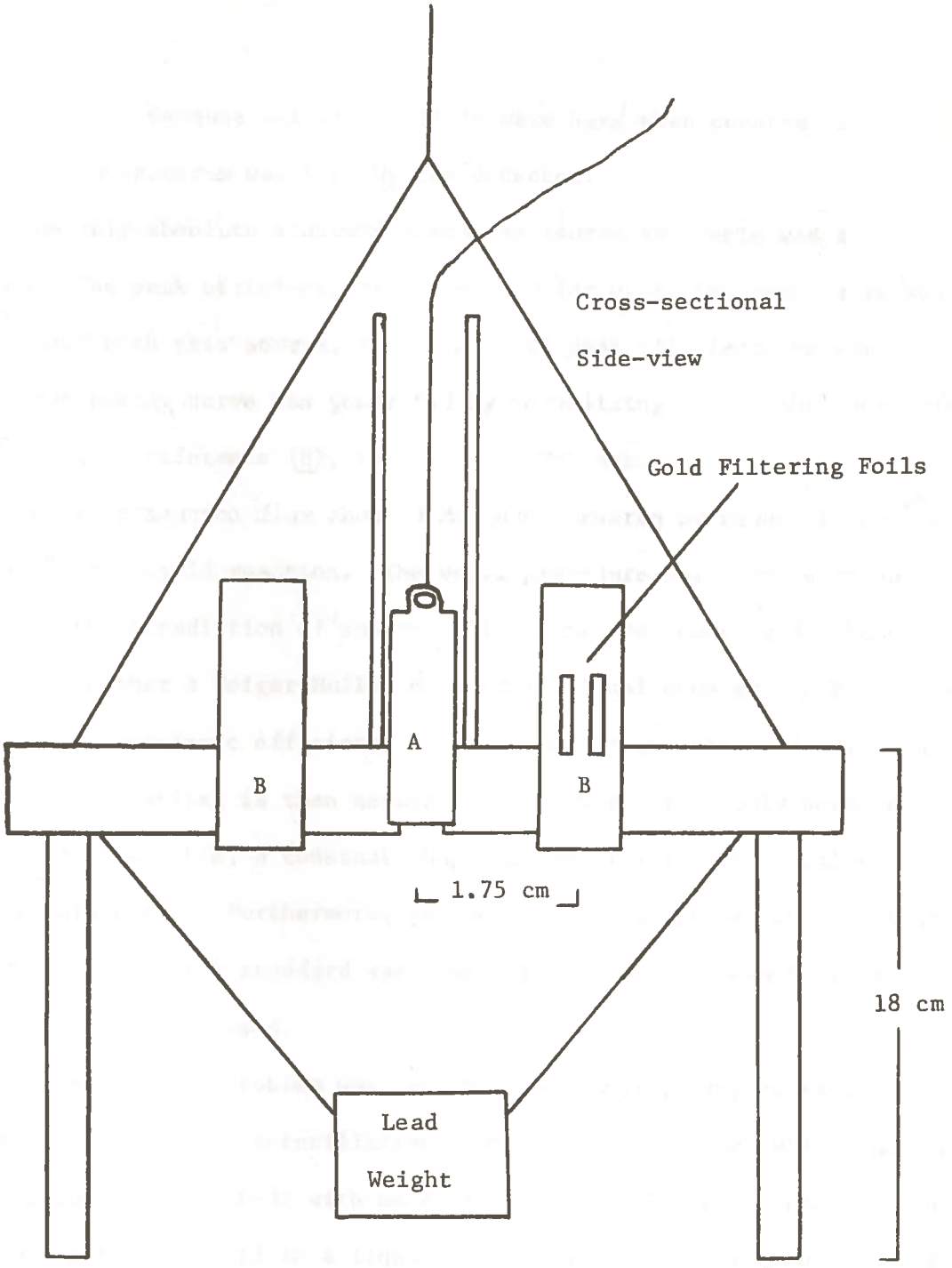

A = Cf-252 source.

B = Irradiation containers, five containing air alone, one containing air, the activation foils, and two gold filtering foils.

FIGURE 9. The Third Irradiation System (Water, Air, and Gold)

centimeters. Because all of the foils were bare when counted, only a pure indium spectrum was seen by the detector.

The only absolute standard gamma-ray source available was a Cs-137 source. The peak efficiency of the system for 0.662 MeV gamma-rays was determined with this source, and a complete peak efficiency versus gamma-ray energy curve was generated by normalizing one of the appropriate curves in reference (8), to the 0.662 MeV datum.

The fast neutron flux about 3 MeV was measured by means of the ^{32}S (n,p) ^{32}P threshold reaction. The usual procedure for this technique involves the irradiation of sulfur pellets and the counting of these pellets with either a Geiger-Muller or a proportional counter. A knowledge of both the intrinsic efficiency of the detector and the self-shielding factor of the pellet is then necessary. However, since only powdered sulfur was available, a constant shape and density for the samples could not be maintained. Furthermore, neither a counter with known efficiency, nor an absolute P-32 standard was available. Thus a somewhat different technique had to be used.

The efficiency problem was overcome by counting samples with a Beckman LS-250 liquid scintillation counter. This machine will count an unquenched sample of P-32 with essentially 100% efficiency. Powdered sulfur does not count well in a liquid scintillation counter because it is not soluble in the liquid scintillation cocktail, and it provides a strong color quench. Consequently, a different sulfur compound had to be used for the measurement. Ethyl disulfide, $(C_2H_5\text{-}S\text{-})_2$, was chosen because of its high sulfur content, organic solubility, low volatility, and lack of color quench. This compound proved to be quite effective, and a

detailed description of the technique in which it was used appears in Appendix C.

A large sample of ethyl disulfide was irradiated in the fast neutron flux measurement because a quench curve had to be determined. Thus the measured fast flux value was actually an average flux value over the relatively large volume of the sample container. A series of approximate correction factors was derived to account for this, the details of which are given in Appendix D.

The fast flux was not measured for the second and third systems because it was felt that neither the air void nor the gold foils would cause a significant perturbation of the fast flux.

CHAPTER IV

DATA COMPARISONS AND CONCLUSIONS

Comparisons of the calculated fast, resonance, and thermal neutron fluxes for the three irradiation arrangements are given in Table I. All fluxes are quoted in units of neutrons-cm^{-2}-sec^{-1} per source neutron.

The resonance flux values should be viewed with some degree of skepticism. It was discovered during the analysis of the measurement data that the flux depression correction factor for the resonance flux was slightly larger than six. Pure indium foils were used since they were available, but there were local variations in foil thickness. This fact coupled with the highly approximate nature of the correction factor itself results in a large variance for the resonance flux value. This extraordinary flux depression could have been avoided by using a combination of regular indium foils and special, low indium content, indium-aluminum foils in the measurement. Unfortunately, no such foils were available when this work was in progress.

As can be seen in Table I, agreement between the calculated and measured thermal fluxes is poor in the first system. This is not expected because system one possesses a very high degree of spherical symmetry and thus should have good agreement between calculation and measurement. This level of agreement is far below that which is generally attributed to a good ANISN calculation for a system well described by a spherically symmetric model. A question thus arises as to whether this discrepancy can be attributed to an error in the code input or an error in the thermal flux measurement.

TABLE I

CALCULATED AND MEASURED NEUTRON FLUXES

All fluxes are in units of neutrons-cm^{-2}-sec^{-1} per source neutron. The thermal, resonance, and fast neutron energies are less than 0.41 ev, approximately equal to 1.45 ev, and greater than 3 Mev respectively.

		System One (Water)	
	Thermal Flux	Resonance Flux	Fast Flux
Calculation	1.54×10^{-2}	1.9×10^{-4}	5.7×10^{-3}
Measurement	$8.5 \times 10^{-3} \pm 15\%$	$1.4 \times 10^{-4} \pm 50\%$	$5.6 \times 10^{-3} \pm 15\%$
Calc./Meas.	1.8	1.35	1.017

		System Two (Air)
	Thermal Flux	Resonance Flux
Calculation	1.0×10^{-2}	1.1×10^{-4}
Measurement	$7.1 \times 10^{-3} \pm 15\%$	$6.5 \times 10^{-5} \pm 50\%$
Calc./Meas.	1.4	1.7

		System Three (Gold)
	Thermal Flux	Resonance Flux
Calculation	1.6×10^{-3}	9.2×10^{-5}
Measurement	$2.1 \times 10^{-3} \pm 15\%$	$8.0 \times 10^{-5} \pm 50\%$
Calc./Meas.	0.76	1.15

A strong case for the validity of the author's calculation can be made through the comparison of calculations shown in Figure 10. The DP-1246 (4) calculation uses an S_{16} angular quadrature, a P_3 angular scattering term expansion, and a 13 group energy structure. The source encapsulation is approximated with a sphere of aluminum having a radius of 0.62 centimeters. The calculation by Nichols (5) uses an S-4 angular quadrature, a 16 group energy structure, a radial mesh spacing varying from 0.2 to 1.0 centimeters, and a source encapsulation approximation identical to that in the DP-1246 calculation. Information on the radial mesh spacing in the DP-1246 calculation and the order of the scattering term expansion in Nichols' calculation is not available.

Nichols' calculation varies significantly from both of the other calculations. This can be attributed to the low order of quadrature that he used. The author's calculated thermal flux is higher than the thermal flux of the DP-1246 calculation by a factor of about 1.15. This can be explained by the lack of an approximation for the source encapsulation and the higher number of energy groups in the author's calculation. Differences in radial mesh spacing, if they exist, could also contribute to this disparity. It should be noted that the two calculations do converge with increasing distance from the source. This is expected since the source encapsulation and radial mesh spacing have their greatest effect near the source. The strong agreement between the author's calculation and the DP-1246 calculation indicates that if errors were made in the author's calculation, then errors were also made in the DP-1246 calculation; and this is most unlikely.

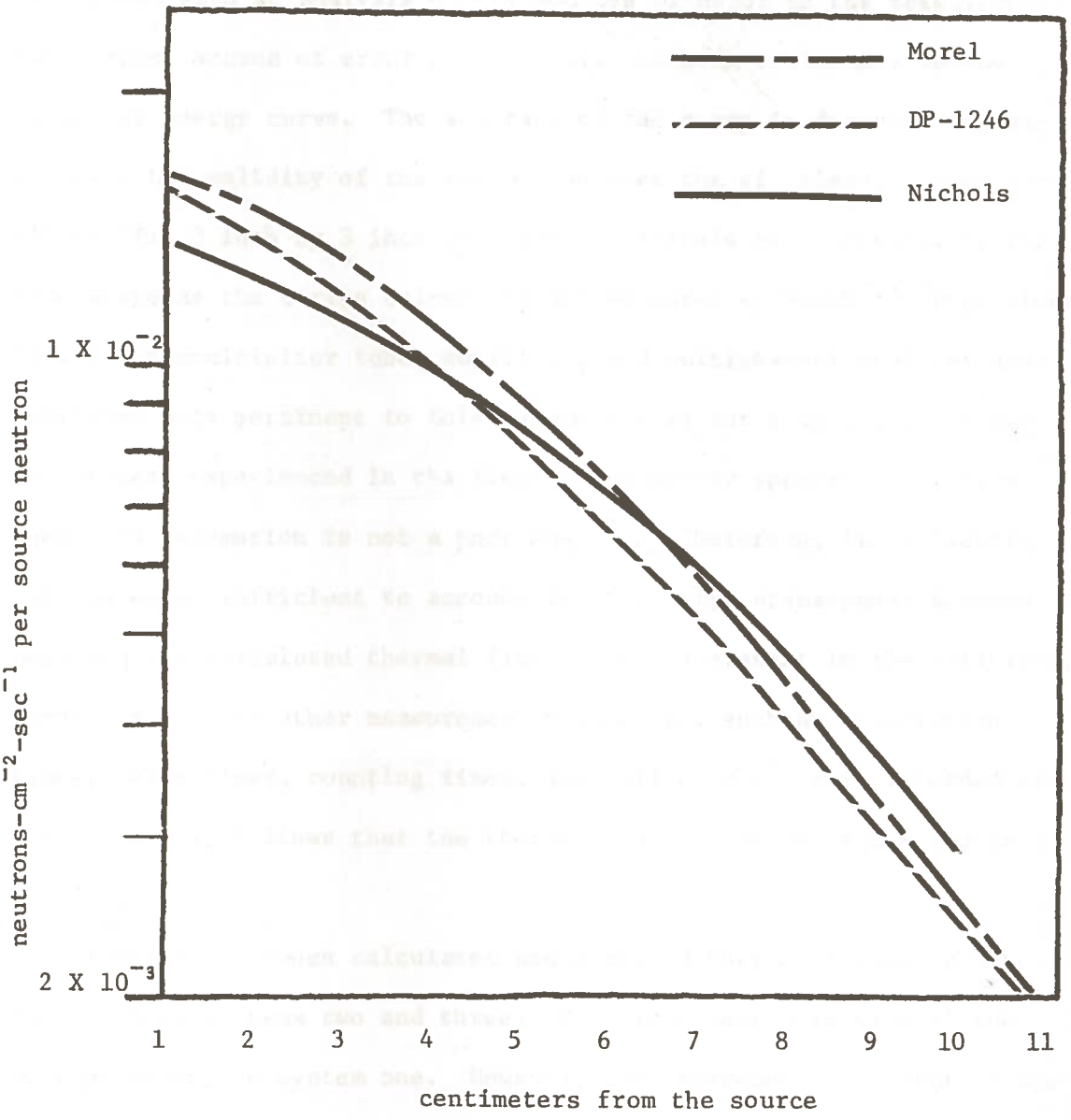

FIGURE 10. A Comparison of ANISN Calculations

The question of error in the thermal flux measurement may be investigated with an analysis of the sources of error in the measurement. The largest source of error was probably the peak efficiency versus gamma-ray energy curve. The accuracy of the curve is directly dependent upon the validity of the assumption that the efficiency curves for all NaI(Tl) 3 inch by 3 inch cylindrical crystals have essentially the same shape as the curves calculated and measured by Heath [8] regardless of the photomultiplier tube, amplifier, and multichannel analyzer used. Published data pertinent to this assumption is not available, but two researchers experienced in the field of gamma-ray spectroscopy claim that this assumption is not a poor one [9]. Therefore, it is doubtful that an error sufficient to account for the large discrepancy between measured and calculated thermal flux values is present in the efficiency curve. Since all other measurement parameters, such as irradiation times, delay times, counting times, and foil weights, were recorded with great care, it follows that the thermal flux measurements are probably quite valid.

Agreement between calculated and measured thermal fluxes is also poor in both systems two and three. This is expected in view of the poor agreement in system one. However, the agreement is better in system two than it is in system one, and the best agreement of all is in system three. This is exactly opposite to what might be expected because each successive system has less spherical symmetry than the preceeding one, and thus, it would seem, should have a poorer agreement. Although it is not immediately obvious, implicit in this argument is the assumption that ANISN can be used to accurately calculate the thermal

neutron flux for all spherically symmetric systems. The results for system one show this assumption to be false. Therefore, the results for systems two and three are not really contradictory. A proper interpretation of these results can be obtained with further data analysis.

The calculated and measured ratios between the thermal neutron fluxes of the three systems are given in Table II. These ratios are important because they are a measure of the relative effect of the air and gold on the unperturbed thermal neutron flux of system one.

ANISN calculated that the spherical air ring would cause a 35% reduction in the thermal neutron flux at 1.75 centimeters from the source. The reduction in thermal neutron flux due to the cylindrical air ring was measured at 16.5%. Unfortunately, this result is somewhat ambiguous because it can be interpreted in any of the following three manners:

(a) ANISN properly calculated the thermal neutron flux perturbation for a 50 cc spherical air ring. The 50 cc cylindrical air ring only caused about one-half of the pertubation that the spherical air ring did because of the different spatial distribution of the air about the source.

(b) The spherical air ring and the cylindrical air ring essentially caused the same thermal neutron flux perturbation, but ANISN overestimated the perturbation caused by the air ring.

(c) Some combination of the explanations described above could also be appropriate.

TABLE II

THERMAL FLUX RATIOS

	System Two / System One	System Three / System One	System Three / System Two
Calculated	0.65	0.1092	0.16
Measured	0.835	0.247	0.295

The proper explanation cannot be found unless the thermal neutron flux perturbation for a 50 cc spherical air ring is measured. Unfortunately, spherical shields and voids are extremely difficult to construct, but if possible, future work with the ANISN code should include such a measurement.

The seemingly strange results of systems two and three can now be explained by the fact that the ANISN code calculated a much greater thermal neutron flux perturbation for the two systems than actually occurred. Since the calculated thermal neutron flux for the unperturbed system was too high, the overestimation of the reduction of the thermal neutron fluxes in the perturbed systems brought the calculations and measurements into closer agreement.

Some brighter conclusions can be drawn through the fast neutron flux data in Table I. The agreement between calculation and measurement is very good. The measured fast neutron flux is expected to be slightly less than the calculated fast neutron flux because the liquid scintillation counter does not count an unquenched P-32 sample with absolutely 100% efficiency.

The following general conclusions can be drawn from this work:

1. The thermal neutron flux value at 1.75 centimeters from a point source of Cf-252 in water obtained from a P_3, S_{16}, 23 group ANISN calculation differs significantly from the measured thermal neutron flux value.
2. This large discrepancy can be only slightly reduced by including a metal encapsulation for the source in the ANISN model.

3. Good agreement occurs between the calculated and measured fast fluxes at 1.75 centimeters from a point source of Cf-252 in water.

A possible explanation for the poor thermal neutron flux calculation for system one was obtained through a personal communication between the author and Mr. Wayne Rhodes of the Neutron Physics Division of Oak Ridge National Laboratory. Mr. Rhodes, who is highly experienced in the use of the ANISN code, claims that a P_3 angular scattering term expansion, while generally accepted as the standard expansion order to be used, is actually insufficient when extremely high angle neutron scattering is of dominant importance in a problem. It would seem quite reasonable to assume that high angle neutron scattering does indeed make a significant contribution to the thermal neutron flux near the source in system one. The accuracy of the fast neutron flux for system one serves to support the validity of Mr. Rhodes' explanation because high angle scattering makes essentially no contribution to the fast neutron flux in hydrogenous media. Further ANISN studies should include an analysis of the effect of the angular scattering term expansion order on the thermal flux solution near the source for a point source of Cf-252 in water.

REFERENCES

1. E. Linn Draper, Jr., "Integral Reaction Rate Determinations - Part I: Tailored Reactor Spectrum Preparation and Measurement", Nuclear Science and Engineering, Vol. 46, No. 1, October, 1971..
2. K. D. Lathrop, "Discrete-Ordinates Methods for the Numerical Solution of the Transport Equation", Reactor Technology, Vol. 15, No. 2, Summer 1972.
3. Ward W. Engle, Jr., "A Users Manual for ANISN", Union Carbide Nuclear Company, K-1693, March 30, 1967.
4. D. H. Stoddard, H. E. Hootman, "^{252}Cf Shielding Guide", E. I. du Pont de Nemours and Company, DP-1246, March, 1971.
5. Jere P. Nichols, "Design Data for Cf-252 Neutron Source Experiments", Nuclear Applications, Vol. 4, June, 1968.
6. "Neutron Activation Foils", prepared by Scientific Staff of Reactor Experiments, Inc.
7. Harry M. Murphy, "Summary of Neutron and Gamma Dosimetry Techniques", Air Force Weapons Laboratory, AFWL, TR-66-111, September, 1967.
8. R. L. Heath, Scintillation Spectrometry Gamma-Ray Spectrum Catalogue, Phillips Petroleum Company, Idaho. Operations Office, Vol. 1, 1964.
9. Personal communications with Dr. Frank A. Iddings and Dr. Edgar L. Steele of the LSU Nuclear Science Center.
10. F. R. Mynatt, F. J. Muckenthaler, and P. N. Stevens, "Development of Two-Dimensional Discrete Ordinates Transport Theory for Radiation Shielding", ORNL Report Number CTC-INF-952, Oak Ridge, Tenn., August 11, 1969.

11. Paul F. Zweifel, Reactor Physics, (McGraw-Hill, Inc.), New York, New York, 1973.

12. Paul S. Pickard, "Neutron Cross-Section Collapsing Code-APRIX-I", AMXRD-BNL 12-70, June 1, 1970.

APPENDIX A

THE BOLTZMANN TRANSPORT EQUATION AND THE DISCRETE ORDINATES METHOD

The Boltzmann transport equation simply establishes a mass balance within the differential phase space volume dP. A phase space is a six-dimensional space which describes both the position and momentum of a particle. The geometry most commonly used for this description is shown in Figure A-1. Position is described with the vector $\vec{r}$, while the momentum is described with both the unit vector $\vec{\Omega}$ and the energy E of the particle. Thus dP is equal to $dV d\vec{\Omega} dE$, where dV is equal to dxdydz and $d\vec{\Omega}$ is equal to $\sin\theta d\theta d\phi$.

The following functions must be defined before the Boltzmann transport equation can be introduced.

The function $\Phi(\vec{r},\vec{\Omega},E)$ expresses the neutron angular energy flux.

The function $\sigma_T(E)$ expresses the macroscopic total cross-section.

The function $\sigma_s(E)$ expresses the macroscopic scattering cross-section.

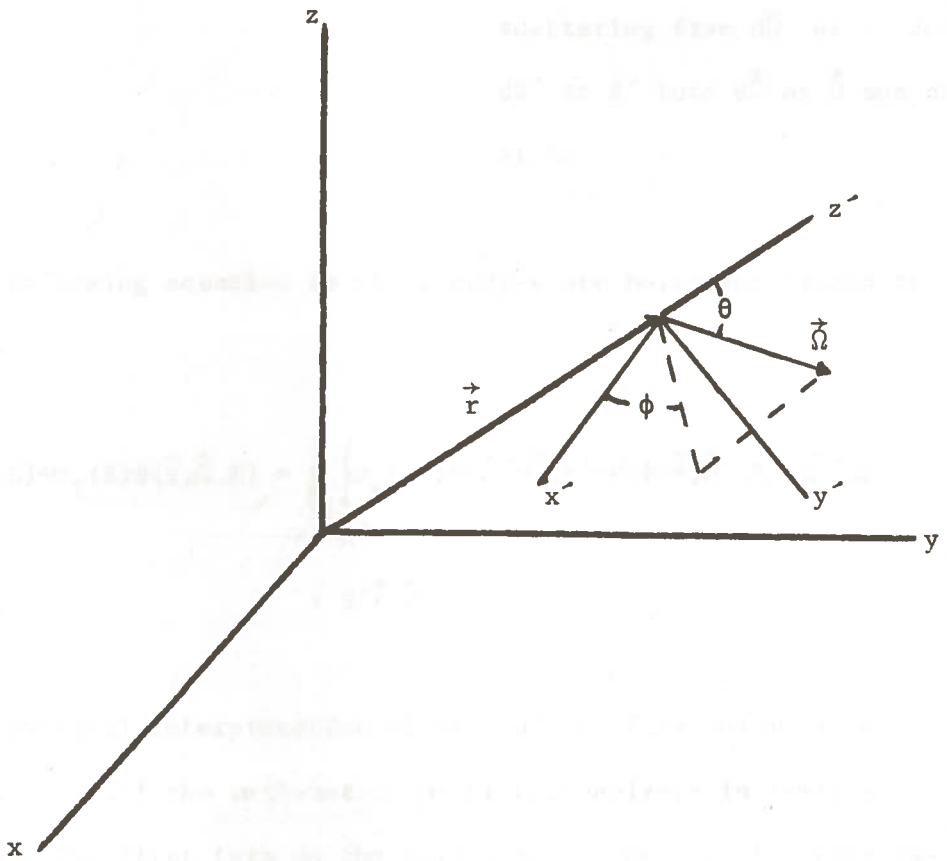

FIGURE A-1. Phase Space Geometry

The function $P(\vec{\Omega}'\rightarrow\vec{\Omega},E'\rightarrow E)\, d\vec{\Omega}'dE'd\vec{\Omega}dE$ expresses the probability per scatter of a neutron within dV scattering from $d\vec{\Omega}'$ at $\vec{\Omega}'$ and dE' at E' into $d\vec{\Omega}$ at $\vec{\Omega}$ and dE at E.

The following equation is the steady-state Boltzmann transport equation.

$$\nabla\cdot\vec{\Omega}\Phi(\vec{r},\vec{\Omega},E)+\sigma_T(E)\Phi(\vec{r},\vec{\Omega},E) = \int_{E'}\int_{\vec{\Omega}'}\sigma_s(E')P(\vec{\Omega}'\rightarrow\vec{\Omega},E'\rightarrow E)\Phi(\vec{r},\vec{\Omega}',E')d\vec{\Omega}'dE' + S(\vec{r},\vec{\Omega},E)$$

The physical interpretation of each of the four terms is very straightforward,if the mathematics of vector analysis is familiar to the reader. The first term on the left side of the equation expresses the leakage rate per unit volume per unit solid angle per unit energy of neutrons leaving the differential volume dV at $\vec{r}$ with directions within $d\vec{\Omega}$ at $\vec{\Omega}$ and energies within dE at E. The second term of the equation expresses the sum of the scattering and absorption rates per unit volume per unit solid angle per unit energy of neutrons within dP at $\vec{r}$, $\vec{\Omega}$,and E. The third term of the equation expresses the scattering rate per unit volume per unit solid angle per unit energy of neutrons within dV at $\vec{r}$ with any energy and direction, which scatter into directions within $d\vec{\Omega}$ at $\vec{\Omega}$ and energies within dE at E. The fourth term of the equation expresses the source rate of neutrons within dP at $\vec{r},\vec{\Omega}$,and E.

Thus the steady-state Boltzmann transport equation mathematically states the following simple physical relationship for the differential phase space volume dP: leakage rate + out-scatter and absorption rate = in-scatter rate + source rate.

For problems with spherical symmetry, the equation reduces to the following form, with $r = |\vec{r}|$ and $u = \cos\theta$.

$$\frac{u}{r^2}\frac{\partial}{\partial r}[r^2\Phi(r,u,E)] + \frac{1}{r}\frac{\partial}{\partial u}[(1-u^2)\Phi(r,u,E)] + \sigma_T(E)\Phi(r,u,E)$$

$$= \int_0^{\infty}\int_{-1}^{+1}\sigma_s(E')P(u'\rightarrow u,E'\rightarrow E)\Phi(r,u',E')du'dE' + S(r,u,E) \qquad (A\text{-}1)$$

This is the equation which is solved by ANISN with the discrete-ordinance method. The first step in the discrete-ordinance method is to choose three sets of discrete variables from the continuous variables of the equation. The set of discrete radial points is known as the radial mesh. The discrete set of direction cosines is known as the angular quadrature, and the set of discrete energy values is known as the energy group structure.

A finite phase space volume is defined for each discrete phase space point by $4\pi r_i^2\Delta r_i 2\pi\Delta u_j\Delta E_k$, where $\Delta r_i = r_{i+1} - r_i$, $\Delta u_j = u_{j+1/2} - u_{j-1/2}$, and $\Delta E_k = E_{k+1/2} - E_{k-1/2}$. The exact relationship between X_a and $X_{a\pm1/2}$ can vary, but the relationship generally used for all three variables is $X_{a+1/2} = 1/2[X_a + X_{a+1}]$.

A mass balance can be established within each finite phase space volume by integrating each term of equation 1 over the volume. The corresponding integral operator T can be defined as a product of three

other integral operators, T_r, T_u, and T_E. These operators are defined as follows.

$$T_r = \int_{r_i}^{r_{i+1}} 4\pi r^2 \, dr$$

$$T_u = \int_{u_{j-1/2}}^{u_{j+1/2}} 2\pi \, du$$

$$T_E = \int_{E_{k-1/2}}^{E_{k+1/2}} dE$$

Thus $T = T_r T_u T_E = \int_{E_{k-1/2}}^{E_{k+1/2}} \int_{u_{j-1/2}}^{u_{j+1/2}} \int_{r_i}^{r_{i+1}} 8\pi^2 r^2 \, drdudE.$

The mean value theorem is used in the application of the operator if an integral cannot be expressed exactly. By the mean value theorem,

$$\int_a^b f(x)\, dx \simeq (b - a)f(c), \text{ where } c \text{ is an element of } [a,b].$$

This approximation becomes exact when f(c) is the average value of f(x) over [a,b]. Thus with this approximation,

$$T[f(r,u,E)] = 8\pi^2 r_{i+1/2}^2 \Delta r_i w_j \Delta E_k f(r_{i+1/2}, u_j, E_k).$$

The expression w_j is equivalent to Δu_j and is called the cosine weight.

An angular quadrature with a total of N discrete cosine values is called an S_N quadrature. Notice that for this derivation,

$$\sum_{j=1}^{N} w_j = 2.$$

Before the integral operator T is applied to the third term of equation 1, the function $\sigma_s(E')P(u'\rightarrow u,E'\rightarrow E)$ is expanded in a Legendre polynomial. Since the probability of scattering from one angle into another one is a function of only the cosine of the angle between them,

$$\sigma_s(E')P(u'\rightarrow u,E'\rightarrow E) = \sum_{\ell=0}^{\infty} \frac{2\ell+1}{2} \sigma_{s\ell}(E',E)P_\ell(u_o), \text{ where,}$$

$$\sigma_{s\ell}(E',E) = \int_{-1}^{+1} \sigma_s(E')P(u_o,E'\rightarrow E)P_\ell(u_o)\, du_o, \text{ and}$$

$$u_o = u'u + (1-u^2)^{1/2}(1-u'^2)^{1/2}.$$

Of course, the expansion is always truncated after a specified number of terms. If N+1 terms are retained, the expansion is called a P_N expansion. For the sake of simplicity, the expansion will be truncated after one term. Thus a P_0 expansion will be used. This expansion is rigorous for isotropic scattering.

The following expression is obtained after substitution of the Legendre expansion into the third term of equation A-1.

$$\int_0^{\infty} \int_{-1}^{+1} \frac{1}{2} \sigma_{so}(E',E)\Phi(r,u',E')\, du'dE'$$

Assuming the use of both an S_J quadrature and an energy group structure of K discrete values, the preceeding expression can be integrated with the mean value approximation to obtain the following result.

$$\sum_{a=1}^{K}\sum_{b=1}^{J} w_b \Delta E_a \frac{1}{2}\sigma_{so}(E_a,E_k)\Phi(r,u_b,E_a)$$

Applying the operator T to both the preceeding expression and the first, second, and fourth terms of equation 1, the following finite-difference form of the Boltzmann transport equation is obtained.

$$w_j \Delta E_k u_j [r_{i+1}^2 \Phi(r_{i+1},u_j,E_k) - r_i^2 \Phi(r_i,u_j,E_k)]$$

$$+ \quad \Delta r_i r_{i+1/2} \Delta E_k [(1-u_{j+1/2}^2)\Phi(r_{i+1/2},u_{j+1/2},E_k) -$$

$$(1-u_{j-1/2}^2)\Phi(r_{i+1/2},u_{j-1/2},E_k)]$$

$$= \quad r_{i+1/2}^2 \Delta r_i w_j \Delta E_k [\sum_{a=1}^{K}\sum_{b=1}^{J} w_b \Delta E_a \frac{1}{2}\sigma_{so}(E_a,E_k)\Phi(r_{i+1/2},u_b,E_k)]$$

$$+ \quad r_{i+1/2}^2 \Delta r_i w_j \Delta E_k \, S(r_{i+1/2},u_j,E_k) \qquad \text{(A-2)}$$

Equation 2 relates the fluxes at the boundries of the volume with the fluxes at the center of the volume. Thus if the fluxes are known at one boundry, the fluxes at both the center and the opposite boundry of the volume are indeterminate. This problem is usually overcome by assuming that the fluxes at the center of the volume are equal to the linear average of the fluxes at the boundries. When this assumption is

made, the fluxes for all the finite phase space volumes of the system can be found with equation A-2 and the proper system boundry conditions. The boundry conditions corresponding to a point source of neutrons surrounded by a sphere of material with radius R are:

$$\Phi(0,u,E) = \Phi(0,-u,E), \text{ for all } u, \text{ and}$$

$$\Phi(R,u,E) = 0, \text{ for all } u \leq 0.$$

It should be noted that there are many possible variations in the discrete-ordinates method, and that the method presented here is a very simple one. Furthermore, many points concerning the validity of this method have been overlooked. Rigorous discussions of the discrete-ordinance method and the variations associated with it can be found in References (2), (10), and (11). This appendix is based primarily on Reference (2).

APPENDIX B

AIDS AND INPUT FOR ANISN

The following suggestions should be helpful to users of ANISN.

1. The radial mesh spacing should be chosen such that the flux never varies by more than a factor of two across any single mesh space. If the mesh spacing is chosen such that $1 - \frac{r_i}{r_{i+1}} \exp[\ _T(r_i - r_{i+1})] < 1/2$ for all radii, a satisfactory mesh spacing will usually be obtained.

2. The APRIX-I[13] cross-section collapsing code internally supplies the $2\ell+1$ coefficients.

3. Large quadratures and large scattering term expansions are necessary when large albedos exist within the system.

4. Mesh spacing smaller than 0.2 centimeters can only be used with the ANISN.M version of ANISN. If smaller meshes are used with the older ANISN.R version, the flux solution will not converge.

5. If negative fluxes appear with the use of the mixed mode(linear + step) option, there is probably an error in the cross-sections.

A complete listing of the input deck for the first problem follows.

```
//ANISN1 JOB (260,7011,9,5),'50662 MOREL'
 *SETUP          T1522
// EXEC FORTGLG,PARM.LKED='XREF,LET,LIST,OVLY',
// REGION.GO=(235K,40K),TIME=9
//LKED.SYSIN DD UNIT=TAPE,DSN=ANISN.M.COMPILED,LABEL=(01,SL),
// DISP=(OLD,KEEP),VOL=(PRIVATE,RETAIN,SER=T1522)
//           DD *
 ENTRY MAIN
 OVERLAY LEVEL1
 INSERT PLSNT,FIDO,TP,ADJNT,S804,S805,S814,WOT8,S966
 OVERLAY LEVEL1
 INSERT GUTS,S807,S810,S821,S824,S833,DT,CELL,S851
 OVERLAY LEVEL1
 INSERT FINPR,FINPR1,PUNSH,DTFPUN,FLTFX
 OVERLAY LEVEL2
 INSERT BT,SUMARY,FACTOR
 OVERLAY LEVEL2
 INSERT FEWG,WATE
 OVERLAY LEVEL3(REGION)
//GO.FT01F001 DD UNIT=SYSDA,SPACE=(TRK,(800,100),RLSE),
//     DCB=(RECFM=VBS,LRECL=3516,BLKSIZE=3520,HIARCHY=1)
//GO.FT02F001 DD UNIT=SYSDA,SPACE=(TRK,(800,100),RLSE),
//     DCB=(RECFM=VBS,LRECL=3516,BLKSIZE=3520,HIARCHY=1)
//GO.FT04F001 DD UNIT=SYSDA,SPACE=(TRK,(800,100),RLSE),
//     DCB=(RECFM=VBS,LRECL=3516,BLKSIZE=3520,HIARCHY=1)
//GO.FT08F001 DD UNIT=SYSDA,SPACE=(TRK,(800,100),RLSE),
//     DCB=(RECFM=VBS,LRECL=3516,BLKSIZE=3520,HIARCHY=1)
//GO.FT09F001 DD UNIT=SYSDA,SPACE=(TRK,(800,100),RLSE),
//     DCB=(RECFM=VBS,LRECL=3516,BLKSIZE=3520,HIARCHY=1)
//GO.SYSIN DD *
```

```
CF-252 IN WATER  XSEC FLX-WTD
15$                          1              0              3             16              3
                             1              0              1             90              0             23
                             3              4             26              8              4              0
                             8              0              0              1              0              0
                            25              0              0              0              0              1
                             2              0              0              0              1              0
                             0
16*                     0.0            0.0            .001           0.0            0.0
   0.0                  0.0            1.0            0.0            0.0            .001
 3R0.0                T
14*                                                                                                 00000096
 0 +19084- 5 0 +     0+ 0 0 +31962- 4 0 +87664- 522R+     0+ 0 0 +42090- 6          1
 0 +     0+ 0 0 +54473- 4 0 +24989- 4 0 +15720- 421R+     0+ 0 0 +25601- 8          2
 0 +     0+ 0 0 +70520- 4 0 +26673- 4 0 +16240- 4 0 +30150- 520R+     0+ 0          3
 0 +68869- 9 0 +     0+ 0 0 +11204- 3 0 +37872- 4 0 +16602- 4 0 +42333- 5          4
 0 +90244- 619R+     0+ 0 0 +72607- 9 0 +     0+ 0 0 +15155- 3 0 +75838- 4          5
 0 +48787- 4 0 +16167- 4 0 +51065- 5 0 +10101- 518R+     0+ 0 0 +12177- 8          6
 0 +     0+ 0 0 +22142- 3 0 +11670- 3 0 +56929- 4 0 +18463- 4 0 +80577- 5          7
 0 +25370- 5 0 +46960- 617R+     0+ 0 0 +41242- 8 0 +     0+ 0 0 +35119- 3          8
 0 +21327- 3 0 +90896- 4 0 +16245- 4 0 +59808- 5 0 +26101- 5 0 +81892- 6          9
 0 +14804- 616R+     0+ 0 0 +13346- 7 0 +     0+ 0 0 +42792- 3 0 +24083- 3         10
 0 +11429- 3 0 +11415- 4 0 +21008- 5 0 +77343- 6 0 +33754- 5 0 +10581- 6         11
 0 +18928- 715R+     0+ 0 0 +30699- 7 0 +     0+ 0 0 +44249- 3 0 +22994- 3         12
 0 +14590- 3 0 +18360- 4 0 +18651- 5 0 +34326- 6 0 +12637- 6 0 +55152- 7         13
 0 +17288- 7 0 +30927- 814R+     0+ 0 0 +69767- 7 0 +     0+ 0 0 +44516- 3         14
 0 +24976- 3 0 +17610- 3 0 +34028- 4 0 +43569- 5 0 +44260- 6 0 +81457- 7         15
 0 +29989- 7 0 +13088- 7 0 +41025- 8 0 +73391- 913R+     0+ 0 0 +14572- 6         16
 0 +     0+ 0 0 +44616- 3 0 +20899- 3 0 +14010- 3 0 +25982- 4 0 +51063- 5         17
 0 +65381- 6 0 +66419- 7 0 +12224- 7 0 +45003- 8 0 +19640- 8 0 +61564- 9         18
```

```
0 +11013- 912R+     0+ 0 0 +25428- 6 0 +     0+ 0 0 +44627- 3 0 +18301- 3       19
0 +15115- 3 0 +34913- 4 0 +65950- 5 0 +12961- 5 0 +16596- 6 0 +16859- 7       20
0 +31028- 8 0 +11423- 8 0 +49853- 9 0 +15627- 9 0 +27955-1011R+     0+ 0       21
0 +36713- 6 0 +     0+ 0 0 +44638- 3 0 +11521- 3 0 +10620- 3 0 +33791- 4       22
0 +79947- 5 0 +15102- 5 0 +29680- 6 0 +38002- 7 0 +38605- 8 0 +71050- 9       23
0 +26158- 9 0 +11416- 9 0 +35784-10 0 +64014-1110R+     0+ 0 0 +44200- 6       24
0 +     0+ 0 0 +44646- 3 0 +66231- 4 0 +80153- 4 0 +34685- 4 0 +11522- 4       25
0 +27260- 5 0 +51494- 6 0 +10120- 6 0 +12958- 7 0 +13164- 8 0 +24226- 9       26
0 +89192-10 0 +38925-10 0 +12202-10 0 +21827-11 9R+     0+ 0 0 +50085- 6       27
0 +     0+ 0 0 +44652- 3 0 +66231- 4 0 +97967- 4 0 +55445- 4 0 +27013- 4       28
0 +89733- 5 0 +21230- 5 0 +40103- 6 0 +78818- 7 0 +10092- 7 0 +10252- 8       29
0 +18868- 9 0 +69464-10 0 +30315-10 0 +95026-11 0 +16999-11 8R+     0+ 0       30
0 +56755- 6 0 +     0+ 0 0 +44658- 3 0 +66231- 4 0 +97967- 4 0 +62340- 4       31
0 +43180- 4 0 +21037- 4 0 +69884- 5 0 +16534- 5 0 +31233- 6 0 +61383- 7       32
0 +78594- 8 0 +79841- 9 0 +14694- 9 0 +54098-10 0 +23609-10 0 +74007-11       33
0 +13239-11 7R+     0+ 0 0 +64313- 6 0 +     0+ 0 0 +44666- 3 0 +66231- 4       34
0 +97967- 4 0 +62340- 4 0 +48550- 4 0 +33628- 4 0 +16384- 4 0 +54426- 5       35
0 +12877- 5 0 +24324- 6 0 +47805- 7 0 +61208- 8 0 +62181- 9 0 +11444- 9       36
0 +42132-10 0 +18387-10 0 +57636-11 0 +10311-11 6R+     0+ 0 0 +72879- 6       37
0 +     0+ 0 0 +44674- 3 0 +66231- 4 0 +97967- 4 0 +62340- 4 0 +48550- 4       38
0 +37810- 4 0 +26190- 4 0 +12760- 4 0 +42387- 5 0 +10028- 5 0 +18944- 6       39
0 +37231- 7 0 +47669- 8 0 +48426- 9 0 +89124-10 0 +32811-10 0 +14320-10       40
0 +44887-11 0 +80298-12 5R+     0+ 0 0 +82584- 6 0 +     0+ 0 0 +44684- 3       41
0 +66231- 4 0 +97967- 4 0 +62340- 4 0 +48550- 4 0 +37810- 4 0 +29446- 4       42
0 +20397- 4 0 +99374- 5 0 +33011- 5 0 +78101- 6 0 +14753- 6 0 +28995- 7       43
0 +37125- 8 0 +37715- 9 0 +69410-10 0 +25554-10 0 +11152-10 0 +34958-11       44
0 +62540-12 4R+     0+ 0 0 +93583- 6 0 +     0+ 0 0 +44696- 3 0 +66230- 4       45
0 +97967- 4 0 +62340- 4 0 +48550- 4 0 +37810- 4 0 +29446- 4 0 +22934- 4       46
0 +15885- 4 0 +77393- 5 0 +25709- 5 0 +60825- 6 0 +11490- 6 0 +22581- 7       47
0 +28913- 8 0 +29372- 9 0 +54057-10 0 +19902-10 0 +86854-11 0 +27225-11       48
```

```
 0 +48712-12 3R+     0+ 0 0 +10604- 5 0 +     0+ 0 0 +44708- 3 0 +66231- 4        49
 0 +97968- 4 0 +62340- 4 0 +48550- 4 0 +37810- 4 0 +29446- 4 0 +22934- 4        50
 0 +17860- 4 0 +12371- 4 0 +60274- 5 0 +20022- 5 0 +47371- 6 0 +89483- 7        51
 0 +17587- 7 0 +22517- 8 0 +22875- 9 0 +42099-10 0 +15499-10 0 +67641-11        52
 0 +21203-11 0 +37928-12 2R+     0+ 0 0 +13688- 5 0 +     0+ 0 0 +44739- 3        53
 0 +15232- 3 0 +20886- 3 0 +14870- 3 0 +11581- 3 0 +90190- 4 0 +70240- 4        54
 0 +54704- 4 0 +42603- 4 0 +33179- 4 0 +22982- 4 0 +11197- 4 0 +37195- 5        55
 0 +88000- 6 0 +16623- 6 0 +32670- 7 0 +41831- 8 0 +42495- 9 0 +78207-10        56
 0 +28793-10 0 +12566-10 0 +39389-11 0 +70458-12 0 +     0+ 0 0 +58816- 5        57
 0 +     0+ 0 0 +10795- 2 0 +10736- 2 0 +29369- 3 0 +17093- 3 0 +13312- 3        58
 0 +10368- 3 0 +80742- 4 0 +62882- 4 0 +48972- 4 0 +38140- 4 0 +29704- 4        59
 0 +20575- 4 0 +10024- 4 0 +33299- 5 0 +78783- 6 0 +14882- 6 0 +29248- 7        60
 0 +37449- 8 0 +38043- 9 0 +70016-10 0 +25777-10 0 +11250-10 0 +35263-11        61
 0 +63078-12                                                                    62
3R+     0+ 0 0 +20607- 425R+     0+ 0 0 +45040- 4 0 +21985- 424R+     0+ 0         1
 0 +49495- 4 0 +24808- 4 0 +31065- 523R+     0+ 0 0 +58261- 4 0 +28310- 4         2
 0 +70523- 5 0 +75451- 622R+     0+ 0 0 +13515- 3 0 +67065- 4 0 +28547- 4         3
 0 +63544- 5 0 +67984- 621R+     0+ 0 0 +19854- 3 0 +91743- 4 0 +25260- 4         4
 0 +85689- 5 0 +19074- 5 0 +20407- 620R+     0+ 0 0 +43439- 3 0 +14944- 3         5
 0 +15369- 4 0 +39814- 5 0 +13506- 5 0 +30064- 6 0 +32164- 719R+     0+ 0         6
 0 +51222- 3 0 +18306- 3 0 +73927- 5 0 +74695- 6 0 +19350- 6 0 +65639- 7         7
 0 +14611- 7 0 +15632- 818R+     0+ 0 0 +49666- 3 0 +24491- 3 0 +12915- 4         8
 0 +51650- 6 0 +52186- 7 0 +13519- 7 0 +45859- 8 0 +10208- 8 0 +10921- 9         9
17R+     0+ 0 0 +53447- 3 0 +29551- 3 0 +27016- 4 0 +14113- 5 0 +56444- 7        10
 0 +57031- 8 0 +14774- 8 0 +50116- 9 0 +11156- 9 0 +11935-1016R+     0+ 0        11
 0 +45655- 3 0 +24202- 3 0 +19719- 4 0 +17863- 5 0 +93319- 7 0 +37321- 8        12
 0 +37709- 9 0 +97683-10 0 +33137-10 0 +73761-11 0 +78920-1215R+     0+ 0        13
 0 +40308- 3 0 +28365- 3 0 +34367- 4 0 +27748- 5 0 +25136- 6 0 +13131- 7        14
 0 +52517- 9 0 +53063-10 0 +13745-10 0 +46629-11 0 +10380-11 0 +11105-12        15
14R+     0+ 0 0 +25537- 3 0 +21942- 3 0 +43484- 4 0 +52111- 5 0 +42051- 6        16
```

```
0 +38093- 7 0 +19900- 8 0 +79587-10 0 +80413-11 0 +20831-11 0 +70665-12      17
0 +15730-12 0 +16830-1313R+     0+ 0 0 +15692- 3 0 +17175- 3 0 +62577- 4      18
0 +12174- 4 0 +14589- 5 0 +11772- 6 0 +10664- 7 0 +55711- 9 0 +22281-10      19
0 +22513-11 0 +58319-12 0 +19783-12 0 +44036-13 0 +47115-1412R+     0+ 0      20
0 +15692- 3 0 +19691- 3 0 +12367- 3 0 +43008- 4 0 +83667- 5 0 +10027- 5      21
0 +80910- 7 0 +73294- 8 0 +38290- 9 0 +15313-10 0 +15473-11 0 +40082-12      22
0 +13597-12 0 +30265-13 0 +32382-1411R+     0+ 0 0 +15692- 3 0 +19691- 3      23
0 +14659- 3 0 +85001- 4 0 +29559- 4 0 +57504- 5 0 +68913- 6 0 +55609- 7      24
0 +50374- 8 0 +26316- 9 0 +10525-10 0 +10634-11 0 +27548-12 0 +93448-13      25
0 +20801-13 0 +22255-1410R+     0+ 0 0 +15692- 3 0 +19691- 3 0 +14659- 3      26
0 +10075- 3 0 +58421- 4 0 +20316- 4 0 +39521- 5 0 +47363- 6 0 +38219- 7      27
0 +34622- 8 0 +18087- 9 0 +72335-11 0 +73087-12 0 +18934-12 0 +64226-13      28
0 +14297-13 0 +15296-14 9R+     0+ 0 0 +15692- 3 0 +19691- 3 0 +14659- 3      29
0 +10075- 3 0 +69248- 4 0 +40152- 4 0 +13963- 4 0 +27163- 5 0 +32552- 6      30
0 +26268- 7 0 +23795- 8 0 +12431- 9 0 +49716-11 0 +50232-12 0 +13013-12      31
0 +44142-13 0 +98258-14 0 +10513-14 8R+     0+ 0 0 +15692- 3 0 +19691- 3      32
0 +14659- 3 0 +10075- 3 0 +69248- 4 0 +47594- 4 0 +27596- 4 0 +95964- 5      33
0 +18669- 5 0 +22373- 6 0 +18053- 7 0 +16354- 8 0 +85437-10 0 +34169-11      34
0 +34524-12 0 +89434-13 0 +30338-13 0 +67532-14 0 +72255-15 7R+     0+ 0      35
0 +15692- 3 0 +19691- 3 0 +14659- 3 0 +10075- 3 0 +69248- 4 0 +47594- 4      36
0 +32710- 4 0 +18967- 4 0 +65955- 5 0 +12831- 5 0 +15377- 6 0 +12408- 7      37
0 +11240- 8 0 +58719-10 0 +23484-11 0 +23728-12 0 +61467-13 0 +20851-13      38
0 +46414-14 0 +49664-15 6R+     0+ 0 0 +15692- 3 0 +19691- 3 0 +14659- 3      39
0 +10075- 3 0 +69248- 4 0 +47594- 4 0 +32710- 4 0 +22482- 4 0 +13035- 4      40
0 +45330- 5 0 +88184- 6 0 +10568- 6 0 +85279- 8 0 +77251- 9 0 +40357-10      41
0 +16140-11 0 +16308-12 0 +42246-13 0 +14331-13 0 +31900-14 0 +34127-15      42
5R+     0+ 0 0 +33705- 3 0 +44425- 3 0 +31659- 3 0 +21760- 3 0 +14955- 3      43
0 +10279- 3 0 +70643- 4 0 +48553- 4 0 +33369- 4 0 +19348- 4 0 +67284- 5      44
0 +13089- 5 0 +15686- 6 0 +12658- 7 0 +11466- 8 0 +59902-10 0 +23957-11      45
0 +24206-12 0 +62707-13 0 +21271-13 0 +47349-14 0 +50657-15 5R+     0+ 0      46
```

```
 0 +48557- 3 0 +22144- 3 0 +15220- 3 0 +10460- 3 0 +71892- 4 0 +49410- 4       47
 0 +33960- 4 0 +23340- 4 0 +16041- 4 0 +93012- 5 0 +32345- 5 0 +62923- 6       48
 0 +75407- 7 0 +60849- 8 0 +55121- 9 0 +28796-10 0 +11517-11 0 +11636-12       49
 0 +30144-13 0 +10225-13 0 +22761-14 0 +24352-15                               50
 3R+     0+ 0 0 +25759- 425R+     0+ 0 0 +53138- 4 0 +19508- 424R+     0+ 0      1
 0 +61675- 4 0 +25506- 4 0 -22551- 523R+     0+ 0 0 +84853- 4 0 +30818- 4       2
 0 -47312- 6 0 -12438- 522R+     0+ 0 0 +14876- 3 0 +88402- 4 0 +26494- 5       3
 0 -58401- 5 0 -18342- 521R+     0+ 0 0 +24344- 3 0 +39718- 4 0 -16406- 4       4
 0 -12249- 4 0 -50624- 5 0 -10504- 520R+     0+ 0 0 +44388- 3 0 +17341- 4       5
 0 -27605- 4 0 -12609- 4 0 -59035- 5 0 -19468- 5 0 -35967- 619R+     0+ 0      6
 0 +54408- 3 0 -18159- 6 0 -24232- 4 0 -50166- 5 0 -18912- 5 0 -83260- 6       7
 0 -26273- 6 0 -47206- 718R+     0+ 0 0 +55109- 3 0 +27490- 4 0 -37589- 4       8
 0 -45354- 5 0 -85118- 6 0 -31468- 6 0 -13755- 6 0 -43167- 7 0 -77283- 8       9
17R+     0+ 0 0 +56793- 3 0 +32414- 4 0 -65447- 4 0 -10470- 4 0 -11000- 5      10
 0 -20329- 6 0 -74910- 7 0 -32703- 7 0 -10254- 7 0 -18346- 816R+     0+ 0      11
 0 +53219- 3 0 +45553- 4 0 -51650- 4 0 -12203- 4 0 -16225- 5 0 -16586- 6      12
 0 -30549- 7 0 -11249- 7 0 -49096- 8 0 -15390- 8 0 -27533- 915R+     0+ 0      13
 0 +49503- 3 0 +11770- 3 0 -57154- 4 0 -15459- 4 0 -31970- 5 0 -41395- 6      14
 0 -42133- 7 0 -77561- 8 0 -28556- 8 0 -12463- 8 0 -39067- 9 0 -69887-10      15
14R+     0+ 0 0 +34728- 3 0 +16446- 3 0 -36304- 4 0 -17006- 4 0 -36736- 5      16
 0 -73772- 6 0 -94913- 7 0 -96500- 8 0 -17762- 8 0 -65393- 9 0 -28539- 9      17
 0 -89459-10 0 -16004-1013R+     0+ 0 0 +21063- 3 0 +20274- 3 0 +92652- 5      18
 0 -17774- 4 0 -61325- 5 0 -12640- 5 0 -25202- 6 0 -32374- 7 0 -32906- 8      19
 0 -60564- 9 0 -22297- 9 0 -97312-10 0 -30503-10 0 -54568-1112R+     0+ 0      20
 0 +21063- 3 0 +27329- 3 0 +92759- 4 0 -93183- 5 0 -15742- 4 0 -48935- 5      21
 0 -98845- 6 0 -19645- 6 0 -25216- 7 0 -25628- 8 0 -47168- 9 0 -17365- 9      22
 0 -75786-10 0 -23756-10 0 -42498-1111R+     0+ 0 0 +21063- 3 0 +27329- 3      23
 0 +13219- 3 0 +32381- 4 0 -17286- 4 0 -13413- 4 0 -38824- 5 0 -77224- 6      24
 0 -15309- 6 0 -19641- 7 0 -19959- 8 0 -36735- 9 0 -13524- 9 0 -59023-10      25
 0 -18501-10 0 -33098-1110R+     0+ 0 0 +21063- 3 0 +27329- 3 0 +13219- 3      26
```

```
0 +53326- 4 0 +10434- 5 0 -19544- 4 0 -11145- 4 0 -30669- 5 0 -60290- 6      27
0 -11929- 6 0 -15297- 7 0 -15544- 8 0 -28609- 9 0 -10533- 9 0 -45967-10      28
0 -14409-10 0 -25777-11 9R+    0+ 0 0 +21063- 3 0 +27329- 3 0 +13219- 3      29
0 +53326- 4 0 +11435- 4 0 -13850- 4 0 -18911- 4 0 -91038- 5 0 -24147- 5      30
0 -47043- 6 0 -92943- 7 0 -11914- 7 0 -12106- 8 0 -22281- 9 0 -82029-10      31
0 -35799-10 0 -11222-10 0 -20075-11 8R+    0+ 0 0 +21063- 3 0 +27329- 3      32
0 +13219- 3 0 +53326- 4 0 +11435- 4 0 -93484- 5 0 -19680- 4 0 -16965- 4      33
0 -73472- 5 0 -18965- 5 0 -36692- 6 0 -72407- 7 0 -92796- 8 0 -94283- 9      34
0 -17352- 9 0 -63885-10 0 -27880-10 0 -87395-11 0 -15635-11 7R+    0+ 0      35
0 +21063- 3 0 +27329- 3 0 +13219- 3 0 +53326- 4 0 +11435- 4 0 -93484- 5      36
0 -18352- 4 0 -20721- 4 0 -14570- 4 0 -58780- 5 0 -14866- 5 0 -28609- 6      37
0 -56405- 7 0 -72272- 8 0 -73428- 9 0 -13514- 9 0 -49754-10 0 -21713-10      38
0 -68063-11 0 -12178-11 6R+    0+ 0 0 +21063- 3 0 +27329- 3 0 +13219- 3      39
0 +53326- 4 0 +11435- 4 0 -93484- 5 0 -18352- 4 0 -21008- 4 0 -19409- 4      40
0 -12170- 4 0 -46724- 5 0 -11636- 5 0 -22301- 6 0 -43937- 7 0 -56287- 8      41
0 -57186- 9 0 -10525- 9 0 -38748-10 0 -16910-10 0 -53008-11 0 -94819-12      42
5R+    0+ 0 0 +43689- 3 0 +45881- 3 0 +19695- 3 0 +55413- 4 0 -16265- 4      43
0 -48708- 4 0 -59794- 4 0 -59826- 4 0 -54634- 4 0 -43660- 4 0 -24522- 4      44
0 -38998- 5 0 -21753- 5 0 -41473- 6 0 -81640- 7 0 -10457- 7 0 -10623- 8      45
0 -19552- 9 0 -71982-10 0 -31414-10 0 -98473-11 0 -17614-11 5R+    0+ 0      46
0 +74504- 4 0 -15803- 3 0 -16947- 3 0 -16012- 3 0 -14177- 3 0 -12076- 3      47
0 -10033- 3 0 -81944- 4 0 -66126- 4 0 -47474- 4 0 -24063- 4 0 -82102- 5      48
0 -19625- 5 0 -37181- 6 0 -73111- 7 0 -93619- 8 0 -95109- 9 0 -17504- 9      49
0 -64443-10 0 -28124-10 0 -88157-11 0 -15769-11                               50
3R+    0+ 0 0 +28800- 425R+    0+ 0 0 +49428- 4 0 +27700- 524R+    0+ 0       1
0 +59766- 4 0 -22653- 6 0 -71067- 523R+    0+ 0 0 +82805- 4 0 +78815- 5       2
0 -11184- 4 0 -21401- 522R+    0+ 0 0 +11665- 3 0 -56110- 5 0 -37822- 4       3
0 -15212- 4 0 -21188- 521R+    0+ 0 0 +18598- 3 0 -71393- 4 0 -54738- 4       4
0 -22960- 4 0 -58801- 5 0 -68472- 620R+    0+ 0 0 +25967- 3 0 -15984- 3       5
0 -42906- 4 0 -12586- 4 0 -44454- 5 0 -10204- 5 0 -11139- 619R+    0+ 0       6
```

```
 0 +34902- 3 0 -21470- 3 0 -23379- 4 0 -25414- 5 0 -66820- 6 0 -22785- 6        7
 0 -50926- 7 0 -54633- 818R+    0+ 0 0 +38892- 3 0 -26166- 3 0 -39820- 4        8
 0 -17767- 5 0 -18174- 6 0 -47203- 7 0 -16027- 7 0 -35702- 8 0 -38215- 9        9
17R+    0+ 0 0 +36470- 3 0 -31671- 3 0 -80201- 4 0 -48117- 5 0 -19681- 6       10
 0 -19939- 7 0 -51681- 8 0 -17535- 8 0 -39039- 9 0 -41770-1016R+    0+ 0       11
 0 +41682- 3 0 -23818- 3 0 -60154- 4 0 -60771- 5 0 -32505- 6 0 -13053- 7       12
 0 -13196- 8 0 -34186- 9 0 -11597- 9 0 -25816-10 0 -27622-1115R+    0+ 0       13
 0 +43155- 3 0 -20031- 3 0 -94321- 4 0 -93379- 5 0 -87238- 6 0 -45894- 7       14
 0 -18377- 8 0 -18571- 9 0 -48107-10 0 -16320-10 0 -36328-11 0 -38868-12       15
14R+    0+ 0 0 +37995- 3 0 -32361- 4 0 -10090- 3 0 -16578- 4 0 -14479- 5       16
 0 -13285- 6 0 -69608- 8 0 -27853- 9 0 -28144-10 0 -72909-11 0 -24732-11       17
 0 -55054-12 0 -58903-1313R+    0+ 0 0 +25859- 3 0 +12959- 3 0 -79058- 4       18
 0 -33035- 4 0 -47961- 5 0 -40758- 6 0 -37237- 7 0 -19491- 8 0 -77978-10       19
 0 -78792-11 0 -20411-11 0 -69240-12 0 -15413-12 0 -16490-1312R+    0+ 0       20
 0 +25859- 3 0 +24273- 3 0 -26376- 4 0 -75614- 4 0 -24160- 4 0 -33434- 5       21
 0 -28080- 6 0 -25606- 7 0 -13397- 8 0 -53595-10 0 -54154-11 0 -14029-11       22
 0 -47588-12 0 -10593-12 0 -11334-1311R+    0+ 0 0 +25859- 3 0 +24273- 3       23
 0 +16444- 4 0 -79923- 4 0 -63358- 4 0 -17384- 4 0 -23231- 5 0 -19335- 6       24
 0 -17606- 7 0 -92085- 9 0 -36835-10 0 -37219-11 0 -96417-12 0 -32707-12       25
 0 -72804-13 0 -77894-1410R+    0+ 0 0 +25859- 3 0 +24273- 3 0 +16444- 4       26
 0 -69196- 4 0 -88009- 4 0 -49641- 4 0 -12365- 4 0 -16102- 5 0 -13308- 6       27
 0 -12104- 7 0 -63292- 9 0 -25317-10 0 -25580-11 0 -66267-12 0 -22479-12       28
 0 -50037-13 0 -53536-14 9R+    0+ 0 0 +25859- 3 0 +24273- 3 0 +16444- 4       29
 0 -69196- 4 0 -90650- 4 0 -78193- 4 0 -37381- 4 0 -87211- 5 0 -11139- 5       30
 0 -91571- 7 0 -83210- 8 0 -43502- 9 0 -17400-10 0 -17581-11 0 -45544-12       31
 0 -15449-12 0 -34390-13 0 -36795-14 8R+    0+ 0 0 +25859- 3 0 +24273- 3       32
 0 +16444- 4 0 -69196- 4 0 -90650- 4 0 -85368- 4 0 -63218- 4 0 -27438- 4       33
 0 -61134- 5 0 -76943- 6 0 -62991- 7 0 -57201- 8 0 -29899- 9 0 -11959-10       34
 0 -12083-11 0 -31302-12 0 -10618-12 0 -23636-13 0 -25289-14 7R+    0+ 0       35
 0 +25859- 3 0 +24273- 3 0 +16444- 4 0 -69196- 4 0 -90650- 4 0 -85368- 4       36
```

```
 0 -71018- 4 0 -48522- 4 0 -19793- 4 0 -42656- 5 0 -53089- 6 0 -43323- 7        37
 0 -39319- 8 0 -20550- 9 0 -82193-11 0 -83048-12 0 -21514-12 0 -72978-13        38
 0 -16245-13 0 -17382-14 6R+     0+ 0 0 +25858- 3 0 +24273- 3 0 +16444- 4       39
 0 -69196- 4 0 -90650- 4 0 -85368- 4 0 -71018- 4 0 -55418- 4 0 -36064- 4        40
 0 -14104- 4 0 -29660- 5 0 -36598- 6 0 -29792- 7 0 -27027- 8 0 -14124- 9        41
 0 -56490-11 0 -57078-12 0 -14766-12 0 -50157-13 0 -11165-13 0 -11945-14        42
 5R+     0+ 0 0 +42588- 3 0 +18997- 3 0 -14340- 3 0 -24521- 3 0 -24704- 3       43
 0 -21180- 3 0 -16806- 3 0 -12755- 3 0 -94106- 4 0 -58398- 4 0 -21831- 4        44
 0 -44638- 5 0 -54522- 6 0 -44248- 7 0 -40122- 8 0 -20965- 9 0 -83849-11        45
 0 -84721-12 0 -21947-12 0 -74449-13 0 -16572-13 0 -17730-14 5R+     0+ 0       46
 0 -42591- 3 0 -44860- 3 0 -35794- 3 0 -27258- 3 0 -20156- 3 0 -14614- 3        47
 0 -10451- 3 0 -74012- 4 0 -52036- 4 0 -30866- 4 0 -11009- 4 0 -21810- 5        48
 0 -26324- 6 0 -21287- 7 0 -19291- 8 0 -10078- 9 0 -40308-11 0 -40727-12        49
 0 -10550-12 0 -35789-13 0 -79665-14 0 -85230-15                                50
  T                                                                    00000269
17*          .003553  89R0.0        .278053  89R0.0        .321752
89R0.0       .142231  89R0.0        .174871  89R0.0        .067615
89R0.0       .011925  89R0.0      90R0.0       9CR0.0      90R0.0
90R0.0     90R0.0       90R0.0      90R0.0       90R0.0      90R0.0
90R0.0     90R0.0       90R0.0      90R0.0       90R0.0      90R0.0
90R0.0       T
 3*          F0.0                     T
 1*          F0.0
 4*
   0.0         .1          .12         .14         .17       11.2
   .3        7I.4          1.2         1.2762    7I1.4         2.2
   2.3238    5I2.4         3.0       8I3.2         5.0       8I5.3
   8.0       3I8.4        10.0     18I10.5        20.0       2I20.75
   23.0      5I24.0       30.0
 5*          F0.0
```

```
 6*              0.0          .0244936     .0413296     .0392569     .0400796
   .0643754     .0442097     .1090850     .1371702     .1371702     .1090850
   .0442097     .0643754     .0400796     .0392569     .0413296     .0244936
 7*             -.9902984    -.9805009    -.9092855    -.8319966    -.7467506
   -.6504264    -.5370966    -.3922893    -.1389568     .1389568     .3922893
   .5370966     .6504264     .7467506     .8319966     .9092855     .9805009
 8$          90R          1
 9$                       5
10$           2I          5              8 2I          5            8
11$           4R          0 2I           1             4
12*           4R0.0            .033416      .033416      .033416      .033416
19$                       3
  T            T
/*
//
```

APPENDIX C

A FAST NEUTRON FLUX MEASUREMENT TECHNIQUE USING ETHYL DISULFIDE

The $^{32}S(n,p)^{32}P$ threshold reaction is commonly used for the measurement of fast neutron fluxes above 3 Mev. The problems associated with irradiating and counting powdered sulfur can be avoided by using ethyl disulfide as the target material, and counting the irradiated samples with a liquid scintillation counter.

Ethyl disulfide is a colorless oily liquid with a molecular formula of $(C_2H_5\text{-}S\text{-})_2$, a molecular weight of 122.24 amu, and a density of 0.9926 g/cc. Its boiling point is 153°C at 760 mm of pressure, and it is infinitely soluble in alcohols and ethers. Its only undesirable characteristic is its strong, sweet odor, which is similar to that of the malodorous additive in natural gas.

The following experimental procedure is used.

1. Irradiate about 6 ml of ethyl disulfide in either a polyethylene or glass vial. If a cadmium cover cannot be used, a thermal flux measurement should be made to determine the interference from thermal neutron activations.

2. Number and carefully weigh ten liquid scintillation vials. Then carefully pipette the following amounts of irradiated ethyl disulfide into each vial.

Vial	ml
1	0.1
2	0.2
3	0.3
4	0.4
5	0.5
6	0.6
7	0.7
8	0.8
9	0.9
10	1.0

3. Weigh the vials again to determine the amount of ethyl disulfide actually added to each vial. The weight in grams of each sample should be equal to the volume in millimeters of each sample.

4. Add 15 ml of a liquid scintillation cocktail, such as 4 gm PPO and 5 mg POPOP per liter of toluene, to each vial. Then add the following amounts of toluene.

Vial	ml
1	0.9
2	0.8
3	0.7
4	0.6
5	0.5
6	0.4

7	0.3
8	0.2
9	0.1
10	0.0

5. Count the samples after a delay period of at least 24 hours in order to allow competing reaction products to decay away.

6. Determine the count rate per gram for each sample, and make a plot on semi-log paper of count rate per gram versus sample weight. Extrapolate back to zero grams of sample weight to determine the unquenched count rate per gram of sample.

The fast neutron flux above 3 Mev can then be determined using the standard activation equations, and the following information: the effective cross-section for the $^{32}S(n,p)^{32}P$ reaction is 0.3 barns, the natural abundance of ^{32}S is 95.06%, and the half-life of ^{32}P is 14.3 days.(7)

If a cadmium cover is not used during the irradiation, a correction should be made for the interference of the $^{34}S(n,\gamma)^{35}S$ reaction. The following information is needed: the cross-section for this thermal reaction is 0.26 barns, ^{34}S has a natural abundance of 4.18%, and the half-life of the ^{35}S beta emitter is 87 days.(7)

Data obtained in an actual flux measurement indicates that a 0.1 milliliter sample of ethyl disulfide provides a decrease in counting efficiency of about 2%.

APPENDIX D

A FAST FLUX CORRECTION FACTOR

At points very close to a point source of neutrons in a hydrogenous medium, the fast neutron flux can be closely approximated by the uncollided fast neutron flux. thus the following expression for the fast neutron flux applies in the geometry shown in Figure D-1.

$$\phi(x,y,z) \simeq \frac{S \exp[-\sigma_T (x^2 + y^2 + z^2)^{1/2}]}{4\pi(x^2 + y^2 + z^2)}$$

Where S = the source term in neutrons - sec^{-1}, and

σ = the macroscopic total cross-section.

The following integral expresses the average flux value over the cylinder shown in Figure D-1.

$$\overline{\phi} = \frac{1}{\pi a^2 h} \int_{-h/2}^{+h/2} \int_{-a^2}^{+a^2} \int_{d-(a^2-y^2)^{1/2}}^{d+(a^2-y^2)^{1/2}} \phi\,(x,y,z)\, dx\, dy\, dz$$

If an activation sample is distributed throughout the cylindrical container, it is this average neutron flux which is actually measured. If the value of the fast neutron flux at the center of the container is desired, the appropriate correction factor is expressed as shown below.

$$\frac{\phi(d,0,0)}{\overline{\phi}} = \frac{S \exp[-\sigma_T d]}{4\pi d^2\, \overline{\phi}} = F_c$$

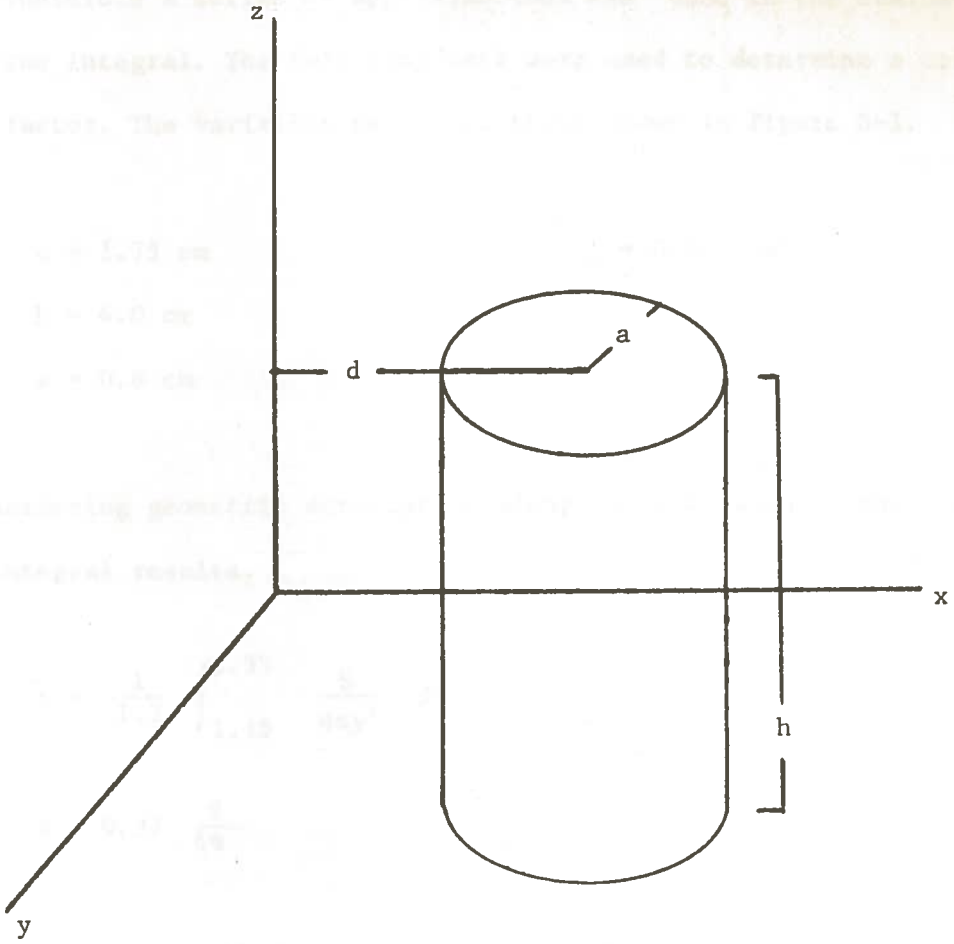

FIGURE D-1. The Geometry Used in the Derivation of the Fast Flux Correction Factor

Unfortunately, the expression for $\bar{\phi}$ cannot be analytically integrated. Therefore a series of approximations was used in the evaluation of the integral. The following data were used to determine a correction factor. The variables relate to those shown in Figure D-1.

$d = 1.75$ cm $\qquad\qquad \sigma_T = 0.182\ \text{cm}^{-1}$

$h = 4.0$ cm

$a = 0.6$ cm

Considering geometric attenuation along the x-axis only, the following integral results.

$$\bar{\phi} = \frac{1}{1.2} \int_{1.15}^{2.35} \frac{S}{4\pi y^2} dy$$

$$\bar{\phi} = 0.37 \frac{S}{4\pi}$$

$$\phi(1.75) = \frac{S}{4\pi(1.75)^2}$$

$$\phi(1.75) = 0.326 \frac{S}{4\pi}$$

$$\frac{\phi(1.75)}{\bar{\phi}} = 0.88 \qquad \text{(D-1)}$$

Considering geometric attenuation along the z-axis only, the following integral results.

$$\bar{\phi} = \frac{1}{2} \int_0^2 \frac{S}{4\pi(1.75^2 + z^2)}\, dz$$

$$\bar{\phi} = \frac{S}{4\pi}\ 0.243$$

$$\frac{\phi(1.75)}{\bar{\phi}} = 1.34 \qquad \text{(D-2)}$$

Considering exponential attenuation along the x-axis only, the following integral results.

$$\bar{\phi} = \frac{1}{1.2} \int_{1.15}^{2.35} \frac{S}{4\pi} \exp[-0.182\ x]\, dx$$

$$\bar{\phi} = \frac{S}{4\pi}\ 0.728$$

$$\phi(1.75) = \frac{S}{4\pi} \exp[-(0.182)(1.75)]$$

$$\phi(1.75) = \frac{S}{4\pi}\ 0.7272$$

$$\frac{\phi(1.75)}{\bar{\phi}} = 0.999 \qquad \text{(D-3)}$$

Considering exponential attenuation along the z-axis only, the following approximate expression results.

$$\bar{\phi} = \frac{S}{4\pi} \frac{[\exp[-(0.182)(1.75)] + \exp[-(0.182)(1.75^2+2^2)^{1/2}]]}{2}$$

$$\bar{\phi} = \frac{S}{4\pi} 0.615$$

$$\frac{\phi(1.75)}{\bar{\phi}} = 1.1795 \qquad \text{(D-4)}$$

Combining factors from D-1, D-2, D-3, and D-4, the following total correction factor results:

$$F_c = (0.88)(1.34)(0.999)(1.1795) = 1.389 \simeq 1.4.$$

The accuracy of this value for the correction factor is not well established. Future work in this area could include an accurate numerical integration of the triple integral expression for $\bar{\phi}$ in order to obtain a more reliable value.

VITA

Jim E. Morel was born on September 22, 1950 in New Orleans, Louisiana. He attended Holy Cross High School in New Orleans, and was graduated in 1968.

In 1968 he entered Louisiana State University and participated in the United States Air Force Reserve Officers Training Corps program. He was graduated with a B.S. in mathematics and was commissioned as a second lieutenant in the United States Air Force Reserve in December 1972.

In January 1973 he began a graduate program at Louisiana State University leading to the degree of Master of Science in Nuclear Engineering.

Upon graduation he will be assigned to active duty in the United States Air Force.